Spectral Estimation Algorithm for Smart Antenna Systems

By

Taufique Ahmed

MS (T&N) 4-B

01-244102-100

Supervised By

Engr. Umar Mujahid

Thesis report is submitted to the Department of Computer Science.
Bahria University, Islamabad.
In partial fulfillment of requirement for the degree of MS (T&N).

CERTIFICATE OF ORIGINALITY

I certify that the intellectual contents of the thesis

"**Spectral Estimation Algorithm for Smart Antenna Systems**"

is the product of my own research work except, as cited properly and accurately in the acknowledgment and references, the material taken from any source such as research papers, research journals, books, internet, etc. solely to support, elaborate, compare and extend the earlier work, Further, this work has not been submitted previously for a degree at this or any other University.

The incorrectness in the above information, if proved at any stage, shall authorize the university to cancel my degree.

Signature: _____. Dated: _____.

Name of the Research student: **Taufique Ahmed.**

ABSTRACT:

The rapid evolution of wireless communication offers enormous attractiveness in the field of smart antenna. Smart antenna systems can be used to enhance channel capacity, bandwidth, signal to noise ratio and MIMO performance. In this technology different directions of arrival (DOA) algorithms have been used for spectral estimation of smart antenna systems i.e. Capon, Bartlett, Liner prediction and MUSIC etc. MUSIC is one of the best algorithms for spectral estimation of smart antenna systems with ULA setup. Also MUSIC algorithm can be used with other array setups.

In this thesis, a detailed study of spectral estimation for smart antenna systems has been conferred. Thesis has been disseminated into two phases; in first phase performance evaluation of the spectral estimation has been accomplished. In the second phase of research, a novel methodology for spectral estimation has been proposed and simulated. Simulation results have shown the significance of the proposed work over the existing spectral estimation techniques.

ACKNOWLEDGEMENTS:

First of all thanks to almighty Allah for giving me determination to complete this thesis. I would like to thanks my supervisor Mr. Umar Mujahid, his assistance and leadership made this project possible. I really admire his teaching and supervision style.

I also want to thanks my parents especially my father who is really a role model for me and supported me for my MS degree.

List of Figures:

List of Tables

Table of Contents

CHAPTER 1

1   INTRODUCTION

1.1   Motivation and Objective

In wireless or mobile communications, users want to access the base station simultaneously and thereby establish the first link in communication chain. The limited resources of base station are distributed among mobile users is via sharing, known as multiple access. Multiple accesses can take place in following ways.

1.1.1 Frequency Division Multiple Access (FDMA)

In FDMA, mobile users are allocated the narrow band of frequency for all the time during communication.

1.1.2 Time Division Multiple Access (TDMA)

In TDMA, entire bandwidth is allocated to each mobile user for a very short period of time.

1.1.3 Code Division Multiple Access (CDMA)

In CDMA, a unique code with access to all bandwidth is allocated to each mobile user for complete duration of call.

There are two main types of CDMA i.e.

> ➢ Direct sequence spread spectrum multiple access
> ➢ Frequency hopped spread spectrum multiple access.

1.1.4 Space Division Multiple Access (SDMA)

In SDMA, geographical area of base station is split into cells where the same carrier frequency can be reused in each cell which increase the capacity. Interference problem is to be considered in SDMA case due to frequency reuse. Introduction of micro and pico cells is one solution to this problem which also adds capacity to personal communication systems. However it was realized that capacity of base stations can be increased further by spatially focusing the transmitted energy along the direction of intended users. In this way transmission can be achieved in same carrier frequency simultaneously with different users. It can be achieved by using an array of antennas at base station and either a switched beam array or tracking beam array can be used to direct the transmitted signals to intended users.

1.2   History

The historical development of adaptive arrays began in late 50s and has been more than four decades in the making. The word adaptive array was first used by Van Atta in 1959, to describe the self-phased array. Self-phased arrays reflect all incident signals back in the direction of arrival by using cleaver phasing schemes based upon

phase configuration. [1] Due to redirection of incident plane waves these arrays are called retro directive arrays. In 1959, Howells proposed side lobe cancellation for the first time. It was the first adaptive technique which allowed for automatic interference nulling, thus increasing the signal to interference level ratio (SNR). Applebaum another scientist developed another algorithm for adaptive interference cancellation. At the same time other methods of adaptive arrays came to existence. In the 60s, phase-lock loop systems are developed for the improvement of retro directive arrays. Because it was assumed that retro direction was the best approach at that time. PLLs are still used in single beam scanning systems. From late 50s to now there is huge advancement in the field of Smart Antenna System. [2]

1.3   <u>What is a Smart Antenna System?</u>

The best definition described by Frank Gross for smart antenna system is "Any antenna array terminated in a sophisticated signal process, which can adapt or adjust its own beam pattern in order to emphasize signal of interest and to minimize interference signals". [3]

A misconception about smart antenna is that it is considered as another type of antenna array and do not realize the signal processing unit. Specific algorithms are used for signal processing for different applications. Main task of signal processing unit are spectral estimation and beamforming to desired users for smart antenna system.

Figure 1- Smart Antenna Systems

Received signals are in analogue form. Different data conversion devices are used to convert the signal into digital form such as analogue to digital converters (ADC) filters and so on to achieve this goal.

1.4 <u>Thesis Outline</u>

In order to understand the spectral estimation algorithms one must have the knowledge of various fields related to smart antenna systems. Most fields related to spectral estimation, smart antenna background and previous research study are covered in this thesis. To cover these disciplines, thesis is categorized as follow;

CHAPTER 1: <u>Introduction</u>

CHAPTER 2: <u>Antenna Basics</u>

CHAPTER 3: <u>Arrays Basics</u>

CHAPTER 4: <u>Channel Characteristics in Wireless Communication</u>

CHAPTER 5: <u>Spectral Estimation Algorithms for Smart Systems</u>

CHAPTER 6: <u>Literature Review and Related Work</u>

CHAPTER 7: <u>Proposed Spectral Estimation Algorithm for Smart Antenna Systems</u>

CHAPTER 8: <u>Conclusion</u>

<div align="center">

CHAPTER 2

2   ANTENNA BASICS

</div>

Spectral estimation of smart antenna system heavily relies on individual antenna behavior. So it is important to analyze the different parameters of an antenna. Some antenna parameters are described in this chapter.

2.1   Antenna Vocabulary

2.1.1 Radiation Pattern

Radiation pattern is the graphical representation describing radiations transmitted or received by an antenna. It can describe electric or magnetic fields known as field pattern or can describe the radiation intensity or power density known as power pattern, both lies in functional description. There are different plot patterns that consist of antenna measurements i.e. polar or Cartesian coordinates. Also radiation patterns can be in linear or logarithmic scales [4]. Figure 2.1 represents the radiation patterns of antenna in polar and rectangular coordinates.

Field pattern
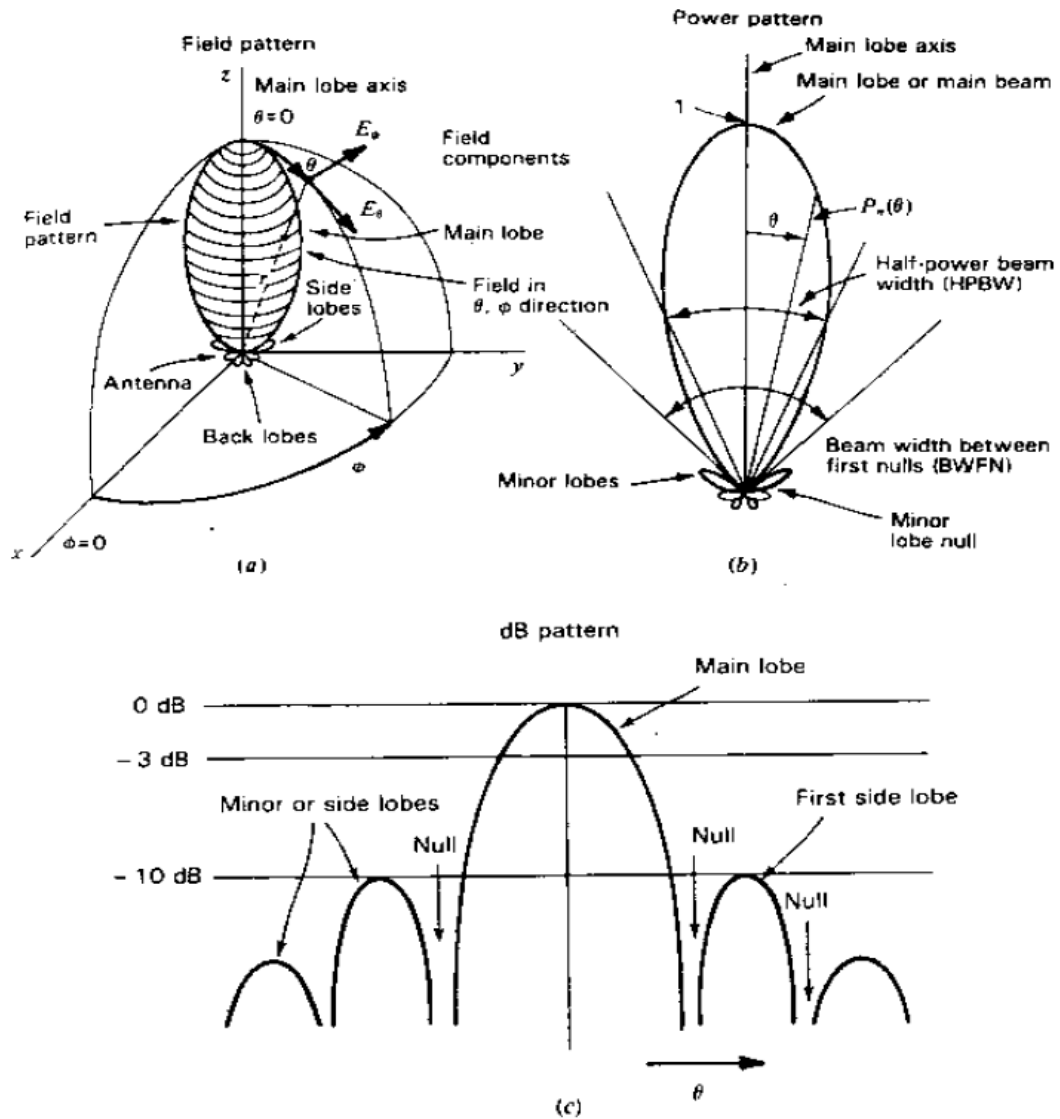
Power pattern

Figure 2- (a) Antenna field pattern with coordinate system. (b) Antenna power pattern in polar coordinates (c) Antenna pattern in rectangular coordinates. [4]

2.1.2 Radiation Regions

The radiation pattern of an antenna changes with respect to distance from antenna which is defined by different radiation regions. Therefore radiation pattern is usually categorized into four regions as explained in [5] and [6].
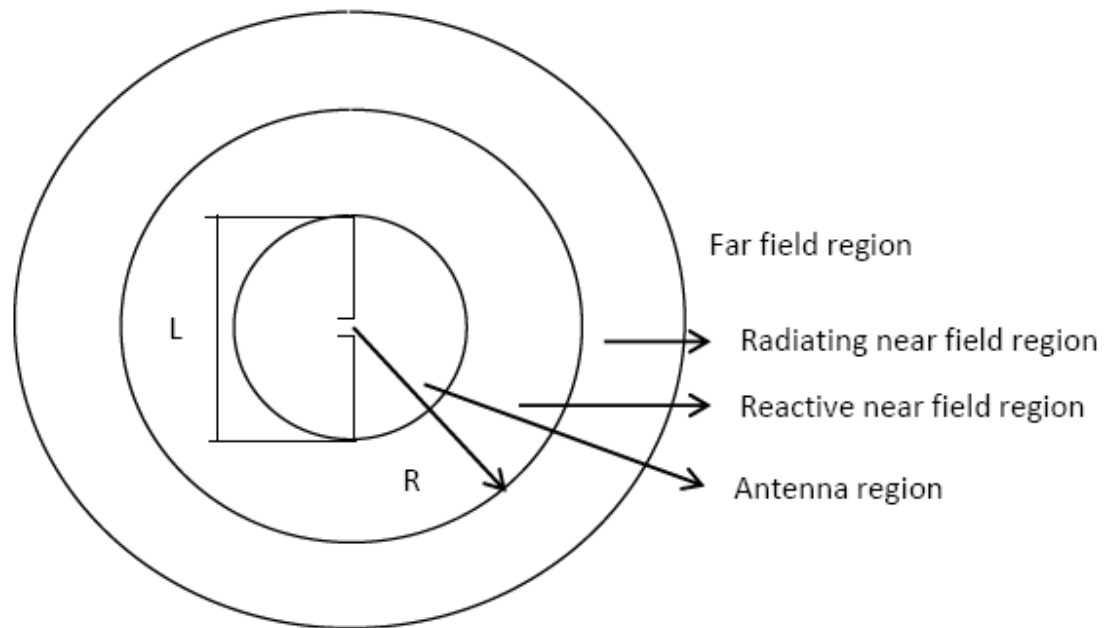
Figure 2- Radiation Regions

L: largest dimension of antenna, R: radius of region

Antenna field region

$$R \leq \frac{L}{2}$$

Reactive near field region

$$R = 0.62\sqrt{\frac{L^2}{\lambda}}$$

Radiating near field region (Fresnel Region)

$$0.62\sqrt{\frac{L^3}{\lambda}} \leq R \leq \frac{L^2}{\lambda}$$

Far field region (Fraunhofer region)

$$R \geq \frac{2L^2}{\lambda}$$

2.1.3 Radiation Power Density

Antennas are the conductors that use to transmit the information wireless through electromagnetic waves. These waves carry power and this is the power which is used

in communication systems. To obtain this power, let us consider the pointing vector, which is given by cross product of electric and magnetic field intensities.

$$\bar{P} = \bar{E} \times \bar{H}$$

And the time varying instantaneous power is given by

$$\bar{P}(r,t) = \bar{E}(r,t) \times \bar{H}(r,t)$$

$$\bar{P}(r,t) = Re\left\{\left(\frac{E_0}{r}\right)e^{j(\omega t - kr)\hat{\theta}}\right\} \times Re\left[\left(\frac{E_0}{\eta r}\right)e^{j(\omega t - kr)\hat{\phi}}\right]$$

$$\bar{P}(r,t) = \left\{\left(\frac{E_0}{r}\right)\cos(\omega t - kr)\hat{\theta}\right\} \times \left[\left(\frac{E_0}{\eta r}\right)\cos(\omega t - kr)\hat{\phi}\right]$$

$$\bar{P}(r,t) = \left\{\left(\frac{E_0{}^2}{2\eta r^2}\right) \times \cos^2(\omega t - kr)\hat{r}\right\}$$

$$\bar{P}(r,t) = \left(\frac{E_0{}^2}{2\eta r^2}\right)[1 + \cos 2(\omega t - kr)\hat{r})]$$

The average power density is given by taking time average of above equation.

$$\bar{W}(r,t) = \frac{1}{T}\int_0^T \bar{P}(r,t)dt$$

$$\bar{W}(r,t) = \left(\frac{E_0{}^2}{2\eta r^2}\right)\bar{r} \qquad (W/m^2)$$

From above equation the average power density is a function of radius and obviously the of electric field.

It can be approved by applying closed surface integral on power density over the sphere boundary of the antenna that

$$\bar{W}(r,t) = \frac{P_{tot}}{4\pi r^2}$$

Where "P_{tot}" is total power radiated by the antenna and "r" is radius of sphere [3].

2.1.4 Radiation Intensity

Radiation power density indicates the power radiated by an antenna at any point but at large distances from antenna it diminishes due to the factor ($\frac{1}{r^2}$). Radiation intensity can be seen as a distance normalized power density. It is given as

$$U(\theta,\phi) = r^2\overline{W}(r)$$

$$U(\theta,\phi) = r^2\frac{P_{tot}}{4\pi r^2}$$

$$U(\theta,\phi) = \frac{P_{tot}}{4\pi}$$

2.1.5 Beamwidth

Usually half power beamwidth is called antenna's beamwidth. The peak radiation intensity is found and the points on either side of the peak which represent half the power of peak intensity are located. The angular distance between the half power points is defined as beamwidth. Half the power expressed in decibels is 3dB, so the half power beamwidth is sometimes referred as 3dB beamwidth. Both horizontal and vertical beamwidths are considered [4].
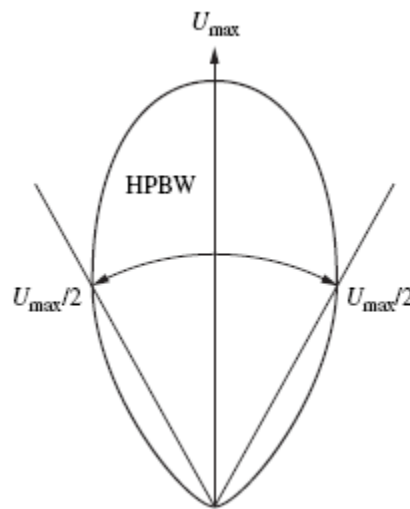
Figure 2- Half power beamwidth [3]

2.1.6 Directivity

It is the degree of measurement of how directive an antenna is relative to isotropic (ideal) antenna radiating the same total power and given by

$$D(\theta,\phi) = \frac{Power\ density\ of\ antenna}{Power\ density\ of\ an\ isotropic\ antenna}$$

So far an isotropic antenna, which radiates in all directions uniformly, its directivity is always equal to 1.

$$D(\theta,\phi) = \frac{W(\theta,\phi)}{P_{tot}/4\pi r^2}$$

$$D(\theta, \phi) = \frac{4\pi \, U \, (\theta, \phi)}{P_{tot}}$$

$$D(\theta, \phi) = \frac{4\pi \, U \, (\theta, \phi)}{\int_{2}^{2\pi} \int_{0}^{\pi} 4\pi \, U \, (\theta, \phi) \sin \theta \, d\theta \, d\phi}$$

The maximum directivity is a constant quantity and is simply maximum of above equation and is denoted by D_0.

$$D_0 = \frac{4\pi \, U_{max}}{\int_{2}^{2\pi} \int_{0}^{\pi} 4\pi \, U \, (\theta, \phi) \sin \theta \, d\theta \, d\phi}$$

2.1.7 Gain

The directivity is an ability of an antenna to direct energy in preferred directions assuming antenna losses. Gain is more practical or real form of directivity including the parameter of efficiency.

$$G(\theta, \phi) = e \, D \, (\theta, \phi)$$

Where "e" is total antenna efficiency. Normally for GSM and DCS indoor Omni antennas gain is around 3 to 5 dB and indoor panel antenna gain is around 7 to 10 dB. Normally for GSM and DCS outdoor panel antennas gain is greater than 17dB.

2.2 <u>Types of Antenna</u>

The types of antenna can be classified upon following broad categories;

2.2.1 Size

The speed of electromagnetic waves is almost same as speed of light, which is given as

$$c = f\lambda$$

Where f = frequency and λ = wavelength

As c is a constant, at specific frequencies the size of antenna has to be specific according to above equation as

$$Size \ of \ antenna = 4 \times \lambda$$

So an antenna can be classified based on its frequency or size.

2.2.2 Directivity

Antenna types considering directivity are

Isotropic Antenna

It is an ideal antenna which radiates it power in all the directions with uniform gain. There is no ideal antenna in this world but we use this antenna type to compare the antenna gain of different types of antenna.

Omni Directional Antenna

It is similar to isotropic antenna which radiates its power in all the direction but not with uniform gain. Radiation pattern of a specific Omni directional antenna with different band of frequencies is shown in below figure.
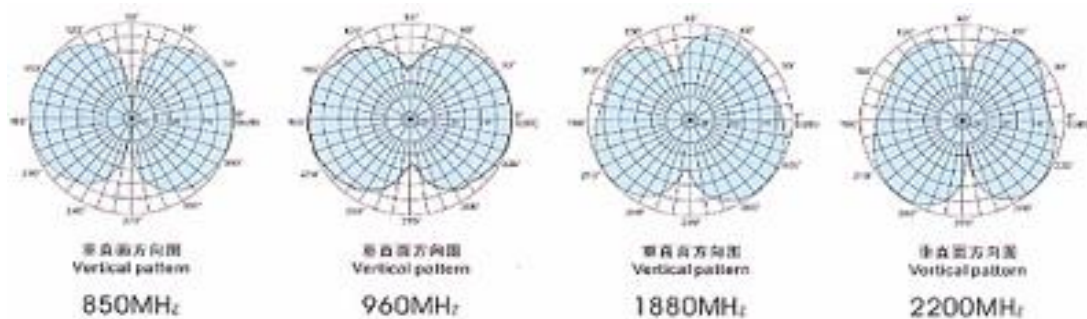
Figure 2- Radiation pattern of Omni directional antennas for different band of frequencies [7]

Directional Antenna

Direction antenna radiates its power in a specific direction. Usually gain of directional antenna is greater than Omni directional antennas as these types of antenna serve in a specific direction. Directional antenna has its main lob in specific direction with maximum directivity along with many side lobes in other directions with less power and directivity. There are further two types of directional antennas i.e. unidirectional and bidirectional antennas. Radiation pattern of a directional antenna is shown below;
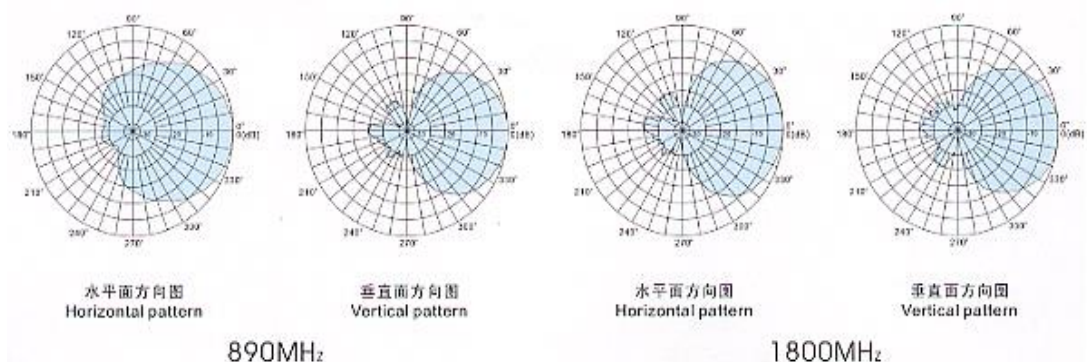
Figure 2- Radiation pattern of panel antenna at different band of frequencies [7]

Antenna Array

Assembly of two or more antenna elements in electrical or geometrical configuration is known as an antenna array. It has large directive gain and can be phasor array, adaptive array and so on.

2.3 Linear Antennas
To understand the complicated structure of antenna arrays used in smart antenna system, it is important to analyze the basis dipole antennas. [6]

2.3.1 Infinitesimal dipole
It is a short wire segment with length $L \ll \lambda$. It is aligned along z-axis symmetrically placed about x-y plane. Using simple mathematical techniques, electric and magnetic fields of infinitesimal dipole can be calculated and form this information, the intensities and directivity can be found as
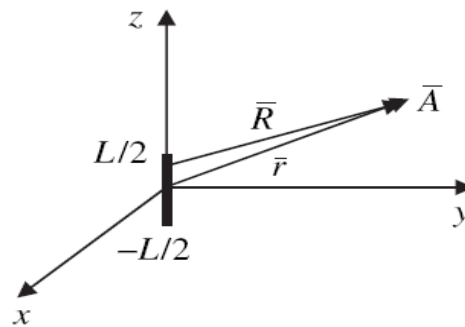
Figure 2- Infinitesimal dipole [6]

Power Density

$$W_r(\theta, \phi) = \frac{\eta}{8} \left| \frac{l_0 L}{\lambda} \right|^2 \frac{sin^2\theta}{r^2}$$

Where "l_0" is the complex phasor current.

Radiation Intensity

$$U(\theta) = \frac{\eta}{8} \left| \frac{l_0 L}{\lambda} \right|^2 sin^2\theta$$

Directivity

$$D(\theta) = \frac{4\pi sin^2\theta}{\int_0^{2\pi} \int_0^{\pi} sin^3\theta \, d\theta \, d\phi} = 1.5 \, sin^2\theta$$

2.3.2 Finite length dipole

Using same mathematical techniques, far field and the intensities and directivity can be calculated as

Power Density

$$W_r(\theta, \phi) = \frac{\eta}{8}\left|\frac{l_0}{\pi r}\right|^2 \left[\frac{\cos\left(\frac{KL}{2}\cos\theta\right) - \cos\left(\frac{KL}{2}\right)}{\sin\theta}\right]^2$$

Radiation Density

$$U(\theta) = \frac{\eta}{8}\left|\frac{l_0}{\pi}\right|^2 \left[\frac{\cos\left(\frac{KL}{2}\cos\theta\right) - \cos\left(\frac{KL}{2}\right)}{\sin\theta}\right]^2$$

Directivity

$$D(\theta) = \frac{4\pi\left[\dfrac{\cos\left(\pi\frac{L}{\lambda}\cos\theta\right) - \cos\left(\pi\frac{L}{\lambda}\right)}{\sin\theta}\right]^2}{\oint_0^{2\pi}\int_0^{\pi}\left[\dfrac{\cos\left(\pi\frac{L}{\lambda}\cos\theta\right) - \cos\left(\pi\frac{L}{\lambda}\right)}{\sin\theta}\right]^2 \sin\theta \ d\theta \ d\phi}$$

2.4 Loop Antennas

2.4.1 Loop of constant phasor current

Loop antenna consists of a wire loop segment having radius a, centered on the z-axis and residing in the x-y plane. We can find the far fields at point r such that a $\ll$ r.

Power Density

$$W_r(\theta, \phi) = \frac{\eta}{8}\left(\frac{2\pi a}{\lambda}\right)^2 \frac{|l_0|^2}{r^2} J^2(\text{ka} \sin\theta)$$

Radiation Density

$$U(\theta) = \frac{\eta}{8}\left(\frac{2\pi a}{\lambda}\right)^2 |l_0|^2 J^2(\text{ka} \sin\theta)$$

Where J_1 is Bessel function of the first kind and order 1.

Directivity

$$D(\theta) = \frac{4\pi J^2(\text{ka} \sin\theta)}{\int_0^{2\pi}\int_0^{\pi} J^2(\text{ka} \sin\theta) \sin\theta \ d\theta \ d\phi}$$

CHAPTER 3

3   ARRAY BASICS

In previous section, the individual antenna characteristics are analyzed. Usually radiation pattern of single element antenna is wide with low directive gain. But for wireless communication high antenna gain is required to meet the long distance communication requirements. Two or more antenna elements are used to achieve this goal. The configuration of antenna elements can be electrical or geometrical (linear, planar and circular) known as antenna array.

For smart antenna systems an adaptive antenna array is considered as it not only increases directive antenna gain but also with the help of spectral estimation algorithms, the exact location of user can be found.

In this section, the discussion of arrays confines to only linear type and array weighting is discussed at the end.

3.1   Linear Arrays

In [8] it is described that Linear arrays are the simplest form of arrays, easy to investigate and useful in understanding the fundamental behavior of other arrays.

3.1.1   Two Element Array

The minimum number of antenna elements in an array is two. Let us consider two antenna elements each of length L, separated by distance d and having electrical phase difference δ. Two elements are placed along x-axis with center zero; one at distance $\frac{d}{2}$ and other at distance $-\frac{d}{2}$ from center. The electric field strength of array is the sum of individual electric field strengths of antenna elements.

$$E_t = E_1 + E_2$$

$$E_t = \frac{jk\eta \, l_0 e^{-j\frac{\delta}{2}}L \sin\theta}{4\pi r} e^{-jkr} + \frac{jk\eta \, l_0 e^{j\frac{\delta}{2}}L \sin\theta}{4\pi r} e^{-jkr}$$

$$E_t = \frac{jk\eta \, l_0 L \sin\theta}{4\pi r} e^{-jkr}[e^{-j\frac{\delta}{2}} + e^{j\frac{\delta}{2}}]$$

$$E_t = \frac{jk\eta \, l_0 L \sin\theta}{4\pi r} e^{-jkr}[e^{-j\frac{(kd \sin\theta + \delta)}{2}} + e^{j\frac{(kd \sin\theta - \delta)}{2}}] \qquad (3.1)$$

Where $k = \frac{2\pi}{\lambda}$
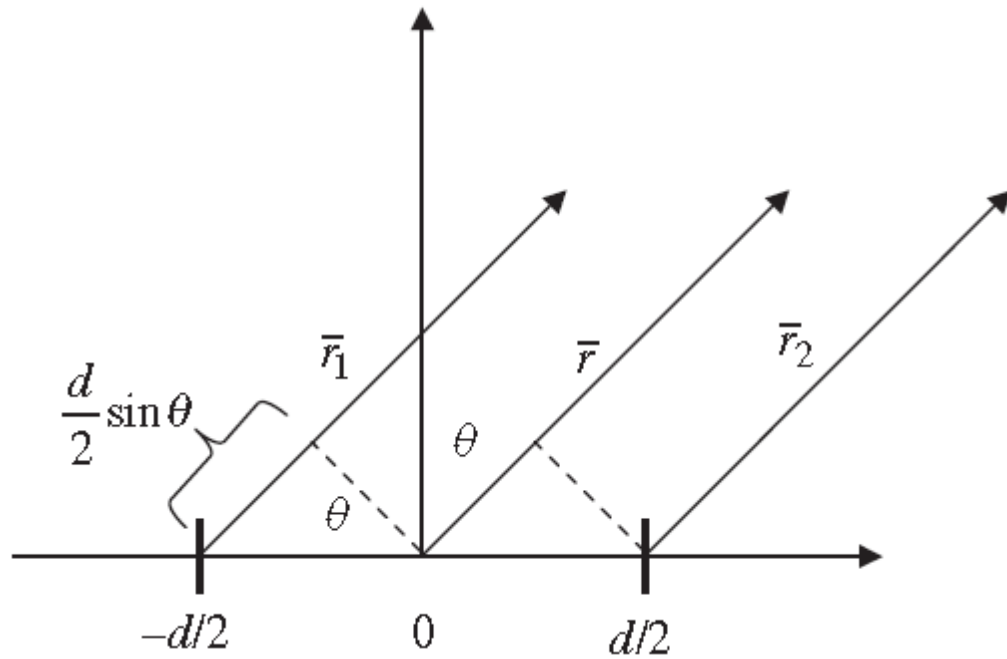
Figure 3- Two infinitesimal dipoles array

Radiation Pattern

The radiation pattern of an array is the product of individual radiation patterns of antenna and array factor.

$$Radiation\ pattern\ (array)$$
$$= (individual\ antenna\ radiation\ patter) \times (array\ factor)$$

From eq. (3.1)

$$E_t = [\frac{jk\eta\ l_0 L \sin\theta}{4\pi r} e^{-jkr}] \times [e^{-j\frac{(kd \sin\theta + \delta)}{2}} + e^{j\frac{(kd \sin\theta + \delta)}{2}}]$$

$$E_t = \left[\frac{jk\eta\ l_0 L \sin\theta}{4\pi r} e^{-jkr}\right] \times [2\cos(\frac{(kd \sin\theta + \delta)}{2})] \quad (3.2)$$

Radiation Intensity

Using eq. (3.2), radiation intensity can be found as

$$U_n(\theta) = [\sin\theta]^2 \times [\cos(\frac{(kd \sin\theta + \delta)}{2})]^2$$

$$U_n(\theta) = [\sin\theta]^2 \times [\cos(\frac{\pi d}{\lambda} \sin\theta + \frac{\delta}{2})]^2$$

Figure 3.2 shows the array factor, individual and total pattern of a dipole antenna array.

(a)

X

(b)

=

(c)
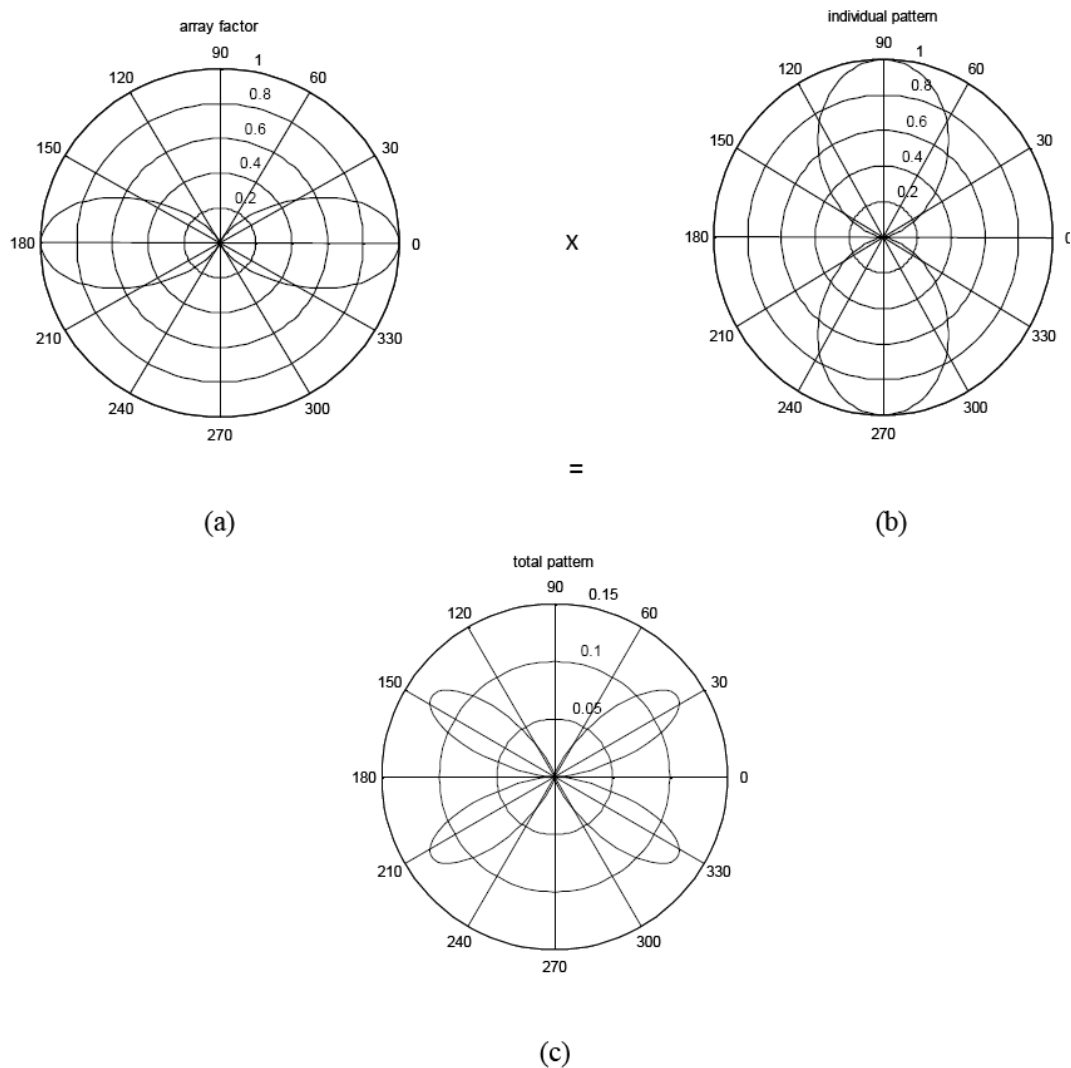
Figure 3- (a) Array factor, (b) individual patterns (c) total pattern [8]

3.1.2 Uniform N-element linear array

In [8] Linear arrays are more generalized having N antenna elements placed at the positive x-axis with equally spaced distance d starting from center to $(N-1)$d. For the sake of simplicity, consider the amplitudes of antenna elements same with the same phase difference δ.

Using the same information as in eq. (3.1), the array factor can be found as

$$AF = 1 + e^{j(kd\sin\theta+\delta)} + e^{2j(kd\sin\theta+\delta)} + \;......\; + e^{(N-1)j(kd\sin\theta+\delta)} \quad (3.3)$$

$$AF = 1 + e^{j\psi} + e^{2j\psi} + \;......\; + e^{(N-1)j\psi}$$

Where $\psi = (kd sine\theta + \delta)$

If array is aligned along z-axis then $\psi = kd\cos\theta + \delta$.
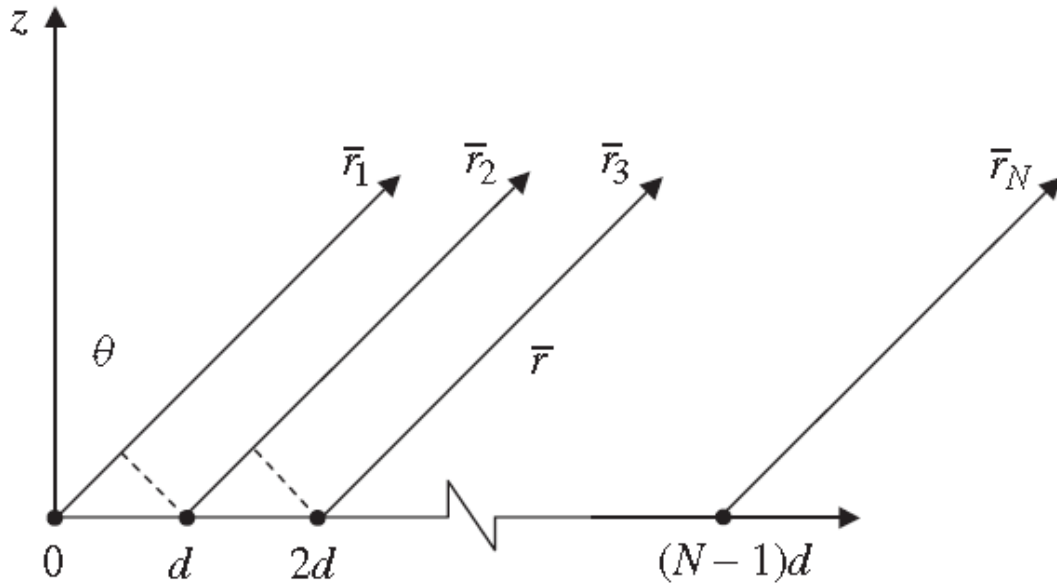
Figure 3- N element liner array

Multiplying both sides with $e^{j\psi}$, we get

$$e^{j\psi}\, AF = e^{j\psi} + e^{2j\psi} + e^{3j\psi} + \,\ldots\ldots\ldots + e^{Nj\psi} \qquad (3.4)$$

Subtracting eq. (3.3) from eq. (3.4) gives

$$\left(e^{j\psi} - 1\right)AF = \left(e^{Nj\psi} - 1\right)$$

$$AF = \frac{\left(e^{Nj\psi} - 1\right)}{\left(e^{j\psi} - 1\right)}$$

$$AF = \frac{e^{j\frac{N}{2}\psi}\left(e^{j\frac{N}{2}\psi} - e^{-j\frac{N}{2}\psi}\right)}{e^{\frac{j}{2}\psi}\left(e^{\frac{j}{2}\psi} - e^{\frac{-j}{2}\psi}\right)}$$

$$AF = e^{j\frac{(N-1)}{2}\psi}\,\frac{\sin(\frac{N}{2}\psi)}{\sin(\frac{\psi}{2})}$$

As the array is placed at center, so above eq. can simplified as

$$AF = \frac{\sin(\frac{N}{2}\psi)}{\sin(\frac{\psi}{2})}$$

And the normalized array factor is given by

$$AF_n = \frac{1}{N}\frac{\sin(\frac{N}{2}\psi)}{\sin(\frac{\psi}{2})}$$

If ψ is very small then $\sin(\frac{\psi}{2}) = \frac{\psi}{2}$, i.e.

$$AF_n = \frac{1}{N}\frac{\sin(\frac{N}{2}\psi)}{\frac{\psi}{2}}$$

$$AF_n = \frac{\sin(\frac{N}{2}\psi)}{\frac{N\psi}{2}} \qquad (3.5)$$

Figure 3.4 shows the plot for above equation.
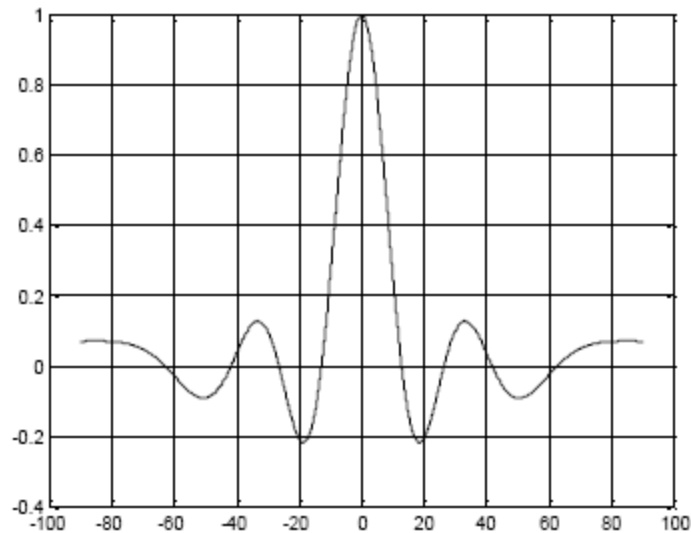
Figure 3- Normalized array factor [8]

Nulls

The argument in eq. (4.5) is very important, nulls occur if

$$\frac{N\psi}{2} = \pm\ n\pi$$

$$\frac{N(kd\sin\theta_{null} + \delta)}{2} = \pm\ n\pi$$

$$\theta_{null} = \sin^{-1}(\frac{1}{kd}(\pm\frac{2n\pi}{N} - \delta)) \qquad for\ n = 1,2,3,\dots$$

Maxima

The main lobe maxima occurs when

$$\frac{\psi}{2} = 0$$

$$\psi = 0$$

$$kd \sin(\theta_{max} + \delta) = 0$$

$$\theta_{max} = -\sin^{-1}(\frac{\delta}{kd})$$

Beamwidth

By definition of beamwidth discussed in CHAPTER 2, we can conclude that

$$\frac{\sin(\frac{N}{2}\psi)}{\frac{N}{2}\psi} = 0.707$$

$$\frac{N}{2}\psi = \pm 1.391$$

$$\frac{N}{2}(kd \sin \theta_\pm + \delta) = \pm 1.391$$

$$\theta_\pm = \sin^{-1}(\frac{1}{kd}(\frac{\pm 2.782}{N} - \delta))$$

And from above equation it can be easily shown that

$$HPBW = |\theta_+ - \theta_-|$$

For large arrays, the half power beamwidth is given as

$$HPBW = 2|\theta_+ - \theta_{max}| = 2|\theta_{max} - \theta_-|$$

Directivity

The directivity of uniform N-element antenna array is given as

$$D(\theta) = \frac{4\pi[\frac{\sin(\frac{N}{2}(kd \cos \theta + \delta))}{\frac{N}{2}(kd \cos \theta + \delta}]^2}{\int_0^{2\pi} \int_0^{\pi} [\frac{\sin(\frac{N}{2}(kd \cos \theta + \delta))}{\frac{N}{2}(kd \cos \theta + \delta}]^2 \sin \theta \, d\theta \, d\phi}$$

The maximum directivity is given by

$$D(\theta) = \frac{4\pi}{\int_0^{2\pi} \int_0^{\pi} [\frac{sin(\frac{N}{2}(kd \cos \theta + \delta))}{\frac{N}{2}(kd \cos \theta + \delta)}]^2 \sin \theta \, d\theta \, d\phi}$$

Beamsteered Linear Array

The variable phase shift δ in an array factor which allows the array to steered towards any direction of interest by putting $\delta = -kd \sin \theta_0$, where θ_0 is the desired angle, from eq. (3.5), by putting value of δ, we get

$$AF_n = \frac{sin(\frac{N}{2}(kd \sin \theta - kd \sin \theta_0))}{\frac{N(kd \sin \theta - kd \sin \theta_0)}{2}}$$

Figure 3.5 shows the plot of 8-element linear array, equally spaced distance of 0.5λ and desired angle $\theta_0 = 45^0$.
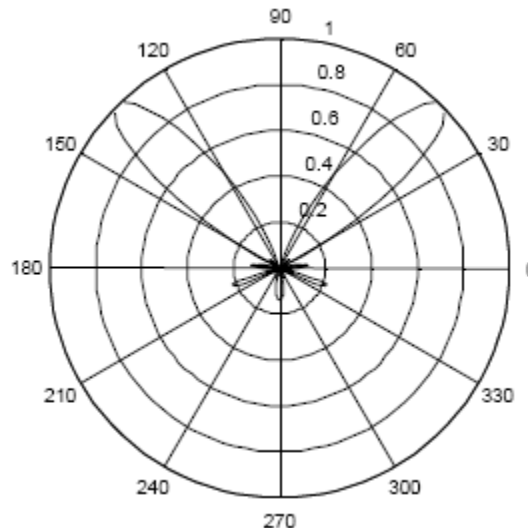
Figure 3- Beamsteered linear array [3]

3.2 Array Weighting

In previous discussion, it was assumed that all the antenna elements have same amplitude and array factor is evaluated accordingly. Figure 3.4 shows the plot of normalized array factor and clearly it can be seen that with mainlobe there are sidelobes as well. These sidelobes shows the power dissipated in the undesired direction. To suppress these sidelobes, weights are assigned to each antenna element of an array. Now array factor is again calculated but with the weights for even number of antenna elements and then for odd number of antenna elements. [9, 10]

Even Array Factor

Let us assume M even antenna elements placed with equally space distance d with each other at positive x-axis from distance $\frac{d}{2}$ to $\frac{(2M-1)d}{2}$. Assign each antenna element a weight from w_1 to w_M.

The array factor now becomes

$$AF_{even} = w_1 e^{j\frac{1}{2}kd\sin\theta} + w_2 e^{j\frac{3}{2}kd\sin\theta} + \cdots + w_M e^{j\frac{(2M-1)}{2}kd\sin\theta}$$

$$AF_{even} = \sum_{n=1}^{M} w_n e^{j\frac{(2n-1)}{2}kd\sin\theta}$$

By taking only the real part from above equation, we get

$$AF_{even} = \sum_{n=1}^{M} w_n \cos(\frac{(2n-1)}{2}kd\sin\theta)$$

And the normalized AF_{even} is given as

$$AF_{even} = \frac{\sum_{n=1}^{M} w_n \cos(\frac{(2n-1)}{2}kd\sin\theta)}{\sum_{n=1}^{M} w_n}$$

Odd Array Factor

Let us assume M+1 odd antenna elements placed with equally spaced distance d along positive x-axis from distance 0 to Md. Assign each antenna element a weight from w_1 to w_{M+1}.

The array factor becomes

$$AF_{odd} = w_1 + w_2 e^{jkd\sin\theta} + + \cdots + w_{M+1} e^{jMkd\sin\theta}$$

$$AF_{odd} = \sum_{n=1}^{M+1} w_n e^{j(n-1)kd\sin\theta}$$

By taking the real part, we get

$$AF_{odd} = \sum_{n=1}^{M+1} w_n \cos((n-1)kd\sin\theta)$$

And the normalized AF_{odd} is given as

$$AF_{odd} = \frac{\sum_{n=1}^{M+1} w_n \cos((n-1)kd\sin\theta)}{\sum_{n=1}^{M+1} w_n}$$

We can plot the modified array factor by substituting weights, from [9, 10] some of the weights are

3.2.1 Binomial weights

Binomial weights are selected from the rows of Pascal's triangle. In MATLAB, it can be calculated with the help of command diag(rot90(pascal(N))). Figure 3.6 shows the plot of binomial weighted array factor superimposed over normal array factor.
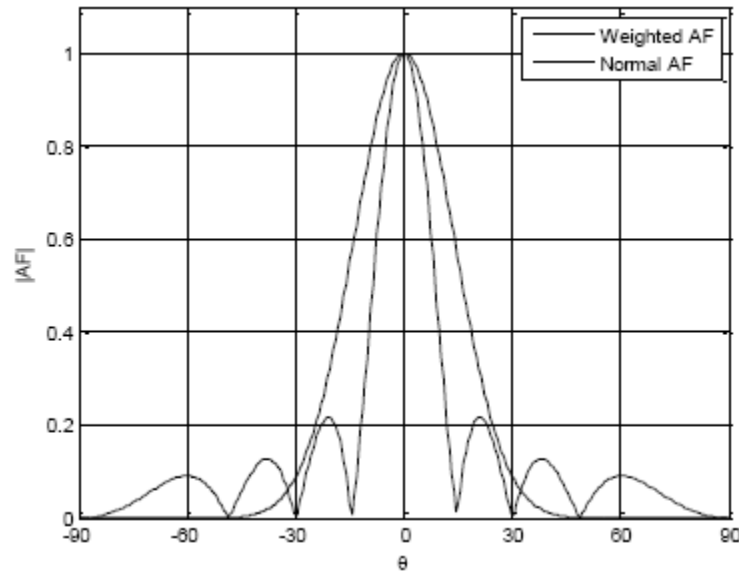
Figure 3- Binomial weighted array factor

3.2.2 Blackman weights

Blackman weights are calculated from

$$w(k+1) = 0.42 - 0.5 \cos(\frac{2\pi k}{(N-1)}) + 0.08 \cos(\frac{4\pi k}{(N-1)}) \quad for \; k = 0,1, \dots N-1$$

Figure 3.7 shows the plot of Blackman weighted array factor superimposed over normal array factor.

3.2.3 Hamming weights

Hamming weights are calculated from

$$w(k+1) = 0.54 - 0.46 \cos(\frac{2\pi k}{(N-1)}) \quad for \; k = 0,1, \dots, N-1$$

Figure 3.8 shows the plot of Hamming weighted array factor superimposed over normal array factor.
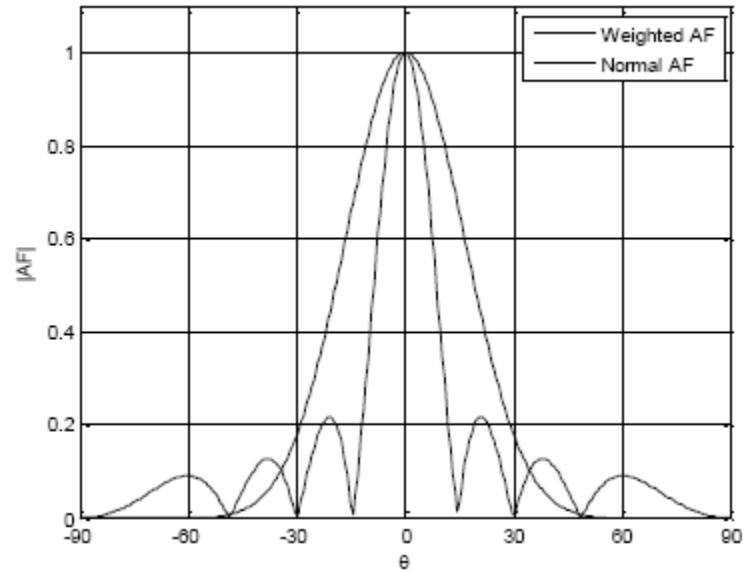
Figure 3- Blackman weighted array factor
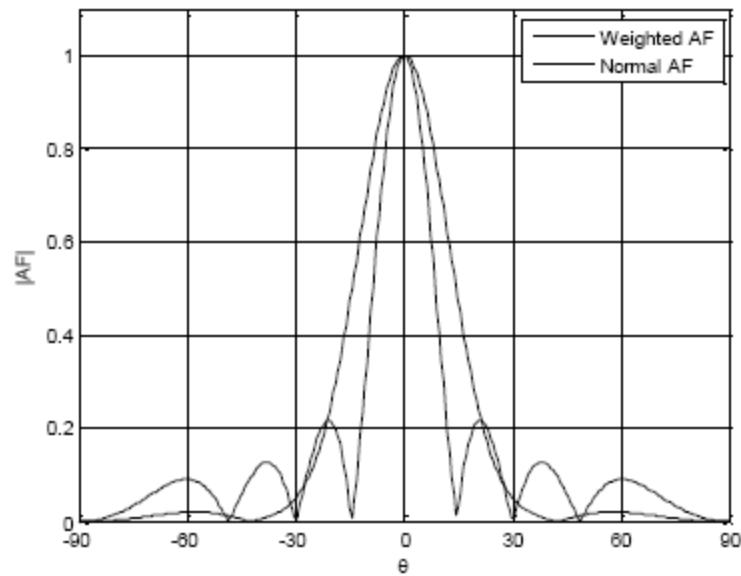
Figure 3- Hamming weighted array factor

3.2.4 Gaussian weights

Gaussian weights are calculated from

$$w(k+1) = e^{\frac{-1}{2}\left(\alpha\frac{k-\frac{N}{2}}{\frac{N}{2}}\right)^2} \quad for \; k = 0,1,\dots,N \; and \; \alpha \geq 2$$

Figure 3.9 shows the plot of Gaussian weighted array factor superimposed over normal array factor.
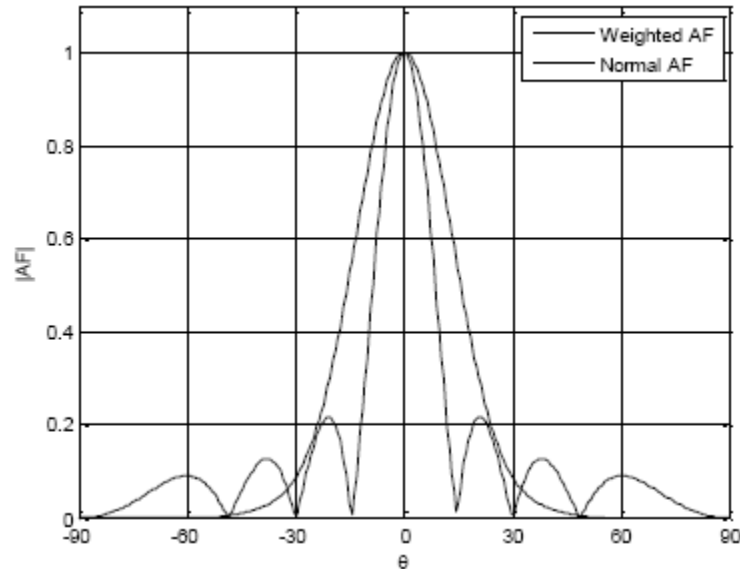
Figure 3- Gaussian weighted array factor

3.2.5 Kaiser-Bessel weights

Kaiser-Bessel weights are calculated from

$$w(k) = \frac{I_0[\pi a \sqrt{\frac{1-(\frac{k}{N})^2]}{2}}}{I_0[\pi a]} \quad for \ k = 0,1,....,\frac{N}{2} \ \ \alpha > 2$$

Figure 3.10 shows the plot of Kaiser-Bessel weighted array factor superimposed over normal array factor.
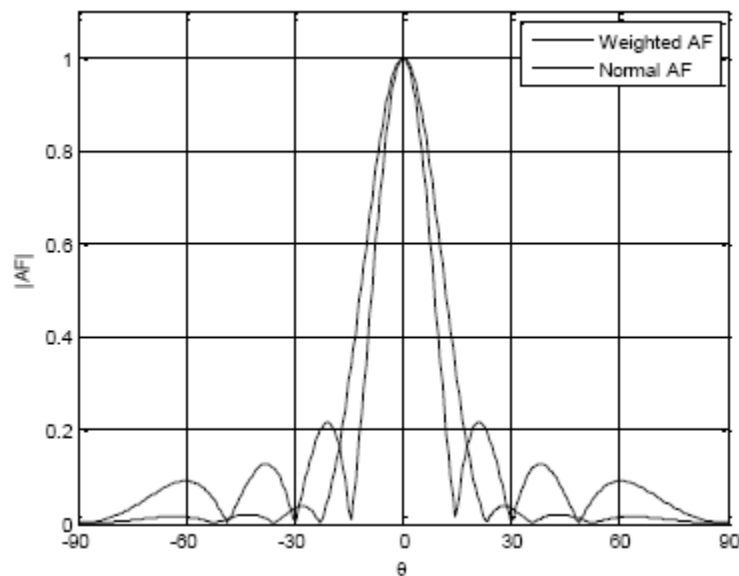
Figure 3- Kaiser-Bessel weighted array factor [3]

CHAPTER 4

4 CHANNEL CHARACTERISTICS IN WIRELESS COMMUNICATION

In wired communication, the channel characteristics are easy to determine and communication is rather simple. But in wireless communication, channel characteristics are heavily dependent upon environment which leads to a complex communication model. Also in wireless communication signal strength is dependent upon many factors like distance between transmitter and receiver, fading and scattering etc. In this section channel characteristics, multipath propagation mechanism and how to improve signal quality are discussed [3].

4.1 Multipath Propagation Mechanisms

A big problem in wireless communication is that the transmitted signals arrive at receivers from multiple paths due to different multipath propagation mechanisms. To sort out this problem, it is necessary to understand these different mechanisms. These mechanisms are explained as under

4.1.1 Reflection

When an electromagnetic signal strikes a smooth surface and reflected back with the same angle, the phenomenon is known as reflection.

4.1.2 Refraction

When an electromagnetic signal strikes a smooth surface and propagates through the surface, the phenomenon is known as refraction.

4.1.3 Scattering

When an electromagnetic signal strikes an object which is much smaller than signal wavelength and signal can spread in any direction, the phenomenon is known as scattering.

4.1.4 Diffraction

When an electromagnetic signal strikes the corner or edge of a structure which is larger than its wavelength, the phenomenon is known as diffraction. Figure 4.1 shows the above mentioned mechanisms. [11]
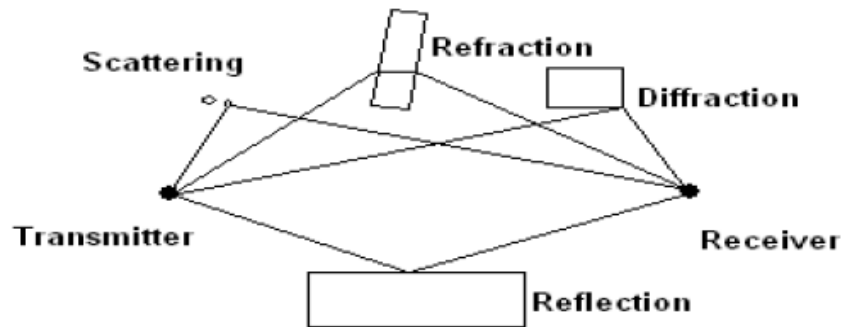
Figure 4- Multipath mechanisms[3]

4.2 Channel Characteristics

The multipath propagation mechanisms discussed earlier are dependent on different obstacles located in environment. In a typical open or outdoor environment, channel characteristics are not certain and depend upon many factors which are of great importance in order to understand the performance of wireless signals.

4.2.1 Fading

Fading is defined as time variation in received signal power due to multipath propagation paths. Fading can classified into fast and slow, also in flat and frequency selective fading.

Fast and Slow Fading

Fast fading is characterized by rapid fluctuations in received signal power over very short distance. It can be observed up to half wavelength distance and known as small-scale fading. Rayleigh and Rician distributions are used for no direct path and direct path respectively in fast fading scenarios.

Slow fading is characterized by slow fluctuations. It can be observed over large distances and thus known as large-scale fading. Log-normal distributions are used in slow a fading scenario, that's why it is known as log-normal fading. Figure 4.2 shows the plots of fast and slow fading.

Flat and frequency selective fading

Flat fading occurs on all frequency components of signal and experience the same magnitude of fading. It is due to the fact that the channel bandwidth is greater than signal bandwidth.

$$B_c > B_s$$

Frequency selective fading occurs on selective frequency components of signal and therefore experience the decorrelated fading. It is due to the fact that the channel bandwidth is smaller than signal bandwidth.
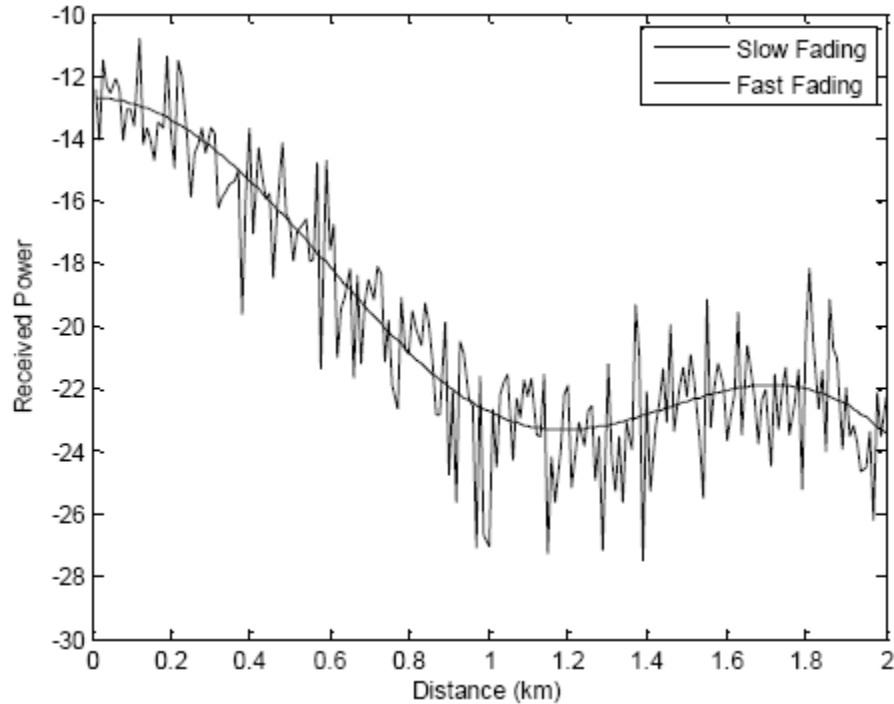
Figure 4- Fast and Slow Fading [3]

4.2.2 Fast Fading Modeling

Let us consider the figure 4.1 with multiple paths with no direct path. The received phasor voltage can be expressed as

$$v_{rs} = \sum_{n=1}^{N} a_n e^{-j(kr_n - \alpha_n)}$$

$$v_{rs} = \sum_{n=1}^{N} a_n e^{j\phi_n}$$

Where

a_n= random amplitude of the nth part

α_n= random phase associated with the nth part

r_n= Length of nth part

$\phi_n = -kr_n + \alpha_n$

The time domain version of the received voltage as

$$v_r = \sum_{n=1}^{N} a_n \cos(\omega_0 t + \phi_n)$$

$$v_r = \sum_{n=1}^{N} a_n \cos(\omega_0 t) \cos(\phi_n) - \sum_{n=1}^{N} a_n \sin(\omega_0 t) \sin(\phi_n)$$

$$v_r = X \cos(\omega_0 t) - Y \sin(\omega_0 t)$$

$$v_r = r \cos(\omega_0 t + \phi)$$

Where

$$X = \sum_{n=1}^{N} a_n \cos(\phi_n)$$

$$Y = \sum_{n=1}^{N} a_n \sin(\phi_n)$$

$$r = \sqrt{X^2 + Y^2}$$

$$\phi = \tan^{-1}\left(\frac{Y}{X}\right)$$

Related to random processes, following are some key points.

1. Random variables X and Y will follow Gaussian distribution with zero mean and standard deviation σ.
2. The envelope r is the result of a transformation of the random variable X and Y and will follow Rayleigh distribution.
3. The phase ϕ will follow a uniform distribution.
4. If the envelop is Rayleigh distribution then it can be shown that the power will follow exponential distribution.

Multipath with direct path

Now let us consider an extra path that is direct path in figure 4.1. The modified phasor voltage is given by

$$v_r = A \cos(\omega_0 t) + \sum_{n=1}^{N} a_n \cos(\omega_0 t + \phi_n)$$

$$v_r = [A + \sum_{n=1}^{N} a_n \cos(\phi_n)] \cos(\omega_0 t) - \sum_{n=1}^{N} a_n \sin(\omega_0 t) \sin(\phi_n)$$

$$v_r = X \cos(\omega_0 t) - Y \sin(\omega_0 t)$$

$$v_r = r \cos(\omega_0 t + \phi)$$

Where

$$X = A + \sum_{n=1}^{N} a_n \, \cos(\phi_n)$$

$$Y = \sum_{n=1}^{N} a_n \, \sin(\phi_n)$$

$$r = \sqrt{X^2 + Y^2}$$

$$\phi = \tan^{-1}(\frac{Y}{X})$$

Related to random processes, following are some key points

1. Random variables X and Y will follow Gaussian distribution with mean of A and standard deviation σ.
2. The envelope r is the result of transformation of the random variables X and Y and will follow Rician distribution.

4.2.3 Channel Impulse Response

A good way to understand the channel characteristics is to find the channel impulse response. But finding the channel impulse response is a complex process. To determine the channel impulse response one must consider following two points;

1. The channel has multipath
2. The channel impulse response is a function of time.

The generalized channel impulse response is given as follows

$$h_c(t,\tau) = \sum_{n=1}^{N} a_n(t)e^{j\psi_n(t)}\delta(\tau,\tau_n(t))$$

Where

$a_n(t)$= time varying amplitude of path n

ψ_n= time varying phase response of path n which can include the effects of Doppler

$\tau_n(t)$= time varying delay of path n

If we assume that the impulse response remains same over the period of time then the channel impulse response can be modified to

$$h_c(\tau) = \sum_{n=1}^{N} a_n e^{j\psi_n}\delta(\tau,\tau_n)$$

4.2.4 Channel Dispersion

Dispersion occurs when the different frequency components of a signal exhibit different propagation velocities. The higher frequency components will propagate at different velocities than lower frequencies which results in different propagation delays and signal degradation at the receiver. Figure 4.3 shows a direct path Gaussian pulse and the received signal for three increasing delay spreads.

4.2.5 Power Delay Profile

Power delay profile gives the power of multipath of a signal at receiver as a function of time delay. It is also known as multipath intensity profile and defined as

$$P(\tau) = E[|h_c(t,\tau)|^2]$$

$$P(\tau) = \sum_{n=1}^{N} P_n \delta(\tau - \tau_n)$$

Where

$$P_n = <|a_n(t)|^2 > | = a_n^2$$

$$\tau_n = <\tau_n(t)>$$

$$<x> = estimate\ of\ the\ random\ varialble\ x$$
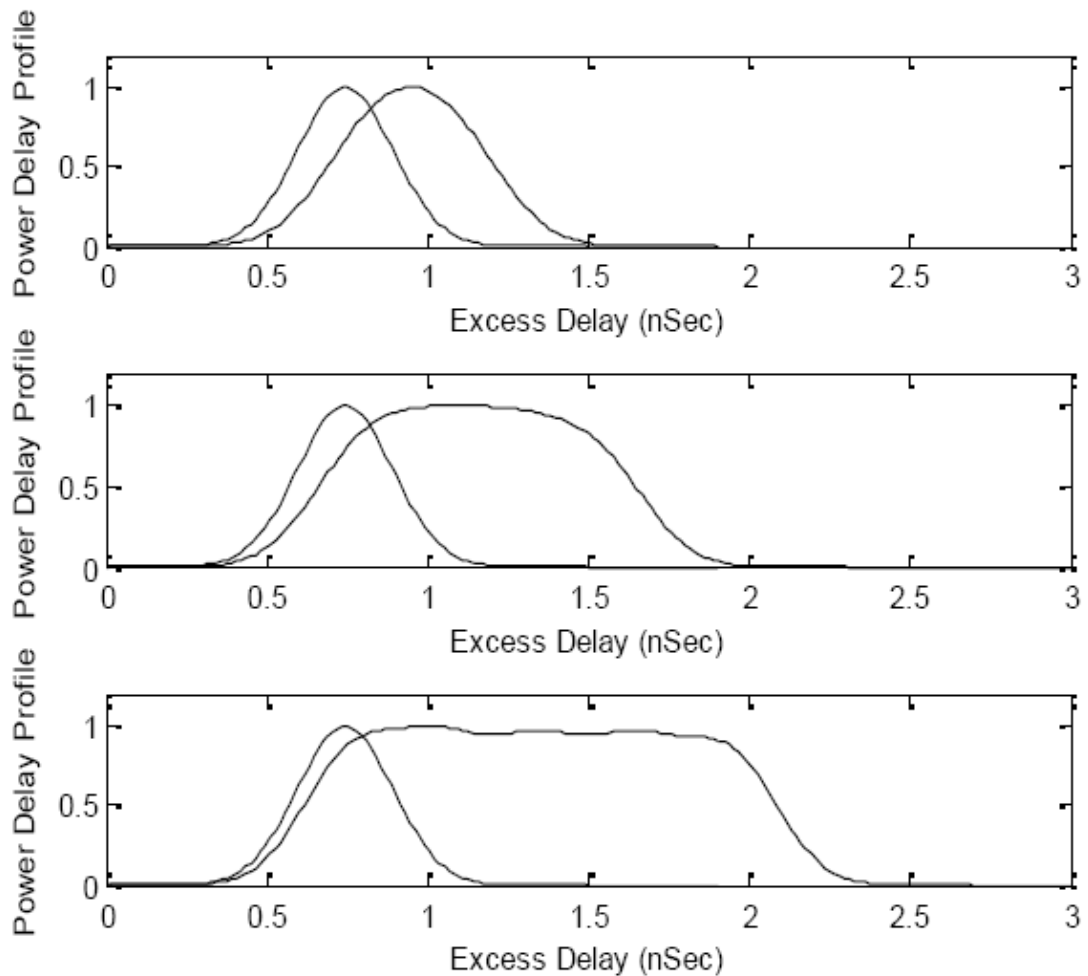
Figure 4- Dispersion caused by delay spread [3]

The signals received at receiver are result of multipath and each signal has different power. Following are the terms used to elaborate power delay profile.

First Arrival Delay τ_n

It is defined as the delay of first time arriving signal. This arriving signal is either the shortest multipath or direct path if a direct path is present. All other delays can be measured relative to first arrival delay. If we consider first arrival delay equal to zero, channel analysis can be simplified.

Excess Delay

It is defined as the additional delay of any multipath signal relative to first arrival delay τ_n.

Maximum Excess Delay

It is defined as the maximum delay of the multipath signal where the power delay profile is above a specified threshold.

Mean Excess Delay (τ_n)

It is defined as the mean value of all excess delays, that is

$$\tau_0 = \frac{\sum_{n=1}^{N} P_n \tau_n}{\sum_{n=1}^{N} P_n}$$

$$\tau_0 = \frac{\sum_{n=1}^{N} P_n \tau_n}{P_T}$$

Where $P_T = \sum_{n=1}^{N} P_n = multipath\ power\ gain$

Root Mean Square Delay Spread (σ_τ)

It is known as the standard deviation for all excess delays, it is define as

$$\sigma_\tau = \sqrt{(\tau^2 + \tau_0{}^2)}$$

$$\sigma_\tau = \sqrt{\frac{\sum_{n=1}^{N} P_n \tau_n{}^2}{P_T} - \tau_0{}^2}$$

4.2.6 Prediction of Power Delay Profiles

To predict the power delay profile, following are the distributions that can be used

One-sided exponential profile

$$P(\tau) = \frac{P_T}{\sigma_\tau} e^{-\frac{\tau}{\sigma_\tau}} \quad \tau \geq 0$$

Gaussian Profile

$$P(\tau) = \frac{P_T}{\sqrt{2\pi\sigma_\tau}} e^{-\frac{1}{2}(\frac{\tau}{\sigma_\tau})^2}$$

Equal amplitude two-ray profile

$$P(\tau) = \frac{P_T}{2} [\delta((\tau) + \delta(\tau - 2\sigma_\tau)]$$

4.2.7 Power Angular Profile

In case of single input single output (SISO), power delay profile is enough for prediction of channel characteristics. But in case of multiple inputs multiple outputs (MIMO), another profile comes to act known as power angular profile. It gives the angular information about the multipath signals and defined as

$$P(\theta) = \sum_{n=1}^{N} P_n \delta(\theta - \theta_n)$$

Following terms are used along with power angular profile to define the angular characteristics of the propagation paths.

Maximum arrival angle (θ_M)

It is the maximum angle relative to the boresight (θ_B) of the receive antenna array.

$$|\theta_M| - \theta_B \leq 180^0$$

Mean arrival angle (θ_0)

It defines the mean value of all arrival angles

$$\theta_0 = \frac{\sum_{n=1}^{N} P_n \theta_n}{\sum_{n=1}^{N} P_n}$$

$$\theta_0 = \frac{\sum_{n=1}^{N} P_n \theta_n}{P_T}$$

Root Mean Square Angular Spread

It is known as standard deviation for all arrival angles

$$\sigma_\theta = \sqrt{(\theta^2 + \theta_0^2)}$$

$$\sigma_\theta = \sqrt{\frac{\sum_{n=1}^{N} P_n \theta_n^2}{P_T} - \theta_0^2}$$

4.2.8 Power Delay-Angular Profile

The combine effect of delay and angular profiles is known as delay-angular profile and given as

$$P(\tau, \theta) = \sum_{n=1}^{N} P_n \delta(\tau - \tau_n) \delta(\theta - \theta_n)$$

Figure 4.4 shows the combine effect of delay and angular profiles.
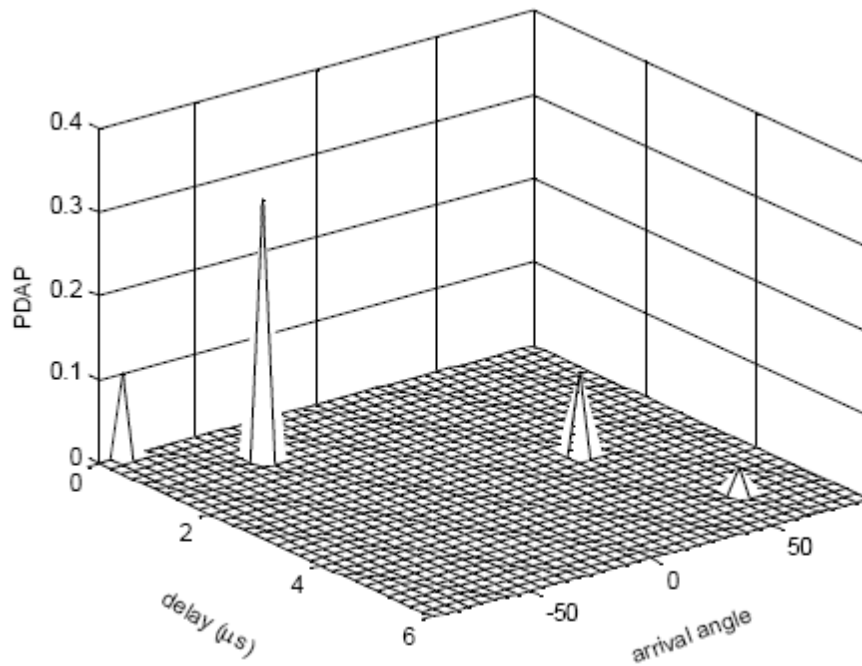
Figure 4- Power delay-angular profile [3]

4.3 **Improving Signal Quality**

The multipath propagation mechanisms and channel characteristics discussed earlier degrade the quality of signal. To improve signal quality, several techniques are used. From [12] some are discussed here

4.3.1 **Equalization**

The main purpose of the equalization is to neutralize the negative effects of the channel by setting the impulse response of equalizer equals to inverse impulse response of channel.

$$H_{eq}(f) = \frac{1}{H_c^*(-f)}$$

If the channel frequency response is characterized by

$$H_c(f) = |H_c(f)|e^{j\phi_c(f)}$$

Then the equalizer frequency response would be given by

$$H_{eq}(f) = \frac{e^{j\phi_c(-f)}}{|H_c(-f)|}$$

As discussed earlier, the channel impulse response is a function of time as well, so the equalizer must be adaptive which can adjust its response according to channel response. Figure 4.4 shows the channel frequency response and equalizer frequency response.
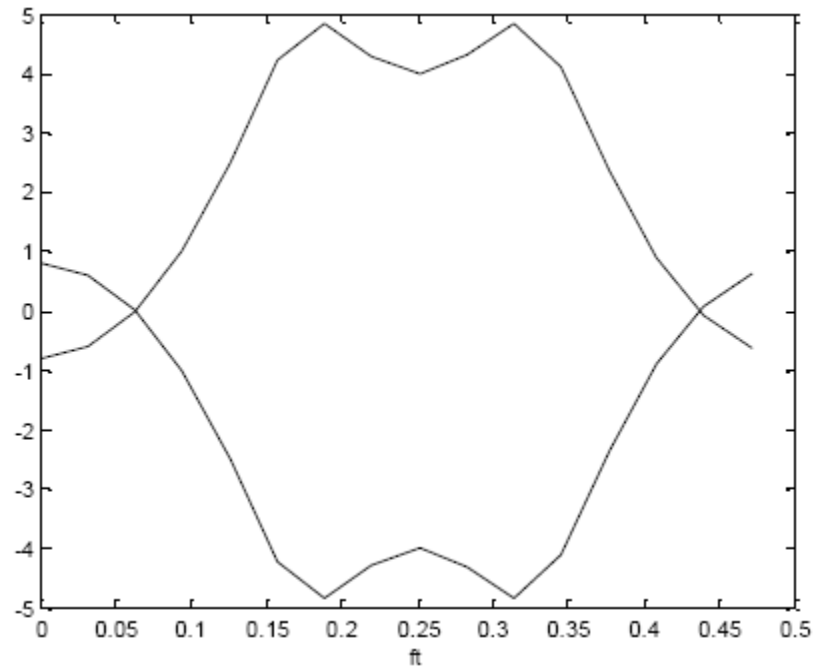
Figure 4- Channel and equalizer frequency response [3]

4.3.2 Diversity

In diversity technique, the replicas of information are transmitted so one having best signal quality can be chosen at the receiver. There are many ways to implement diversity, some of them are;

Space Diversity

Space diversity can be implemented through following four ways

1. Selection diversity
2. Feedback diversity
3. Maximal ratio combining
4. Equal gain combining

Polarization Diversity

Signals having different polarizations are transmitted i.e. Horizontal and vertical etc.

Frequency Diversity

Signals having different frequencies are transmitted.

Time Diversity

Signals having different time delays are transmitted, also known as Code division multiple access (CDMA)

4.3.3 Channel Coding

There are many channel coding schemes that can be used for detection and correction of errors to protect the data from effects of channel. Some channel coding techniques are block codes, convolutional codes, turbo codes and so on.

CHAPTER 5

5 SPECTRAL ESTIMATION ALGORITHMS FOR SMART ANTENNA SYSTEMS

Spectral estimation is mainly known as Angle of Arrival (AOA) estimations. Some other terms are direction of arrival (DOA) estimations and bearing estimations.

In previous section, different multipath propagation mechanisms are discussed and we see that for one transmitter it can be many possible propagation paths and also angle of arrivals. If there are several transmitters operating simultaneously then each transmitter source can create many multipath components at receiver. Therefore the importance of spectral estimation is to find which emitters are present and what are their possible angular locations.

5.1 Array Correlation Matrix

To develop different spectral estimation algorithms, it is necessary to understand the array correlation matrix.[3] Let us consider figure 5.1, in which D signals are arriving from D directions and therefore have different angles of arrivals. These signals are received by M number of antenna elements having M potential weights. Each signal received $x_m(k)$ includes additive white Gaussian noise. The array output can written as

$$y(k) = \bar{w}^T . \bar{x}(k)$$

Where

$$\bar{x}(k) = [\bar{a}(\theta_1 \; \bar{a}(\theta_2) \; \bar{a}(\theta_3 \ldots \ldots \ldots \bar{a}(\theta_D)] . \begin{bmatrix} s_1(k) \\ s_2(k) \\ . \\ . \\ s_D(k) \end{bmatrix} + n(k)$$

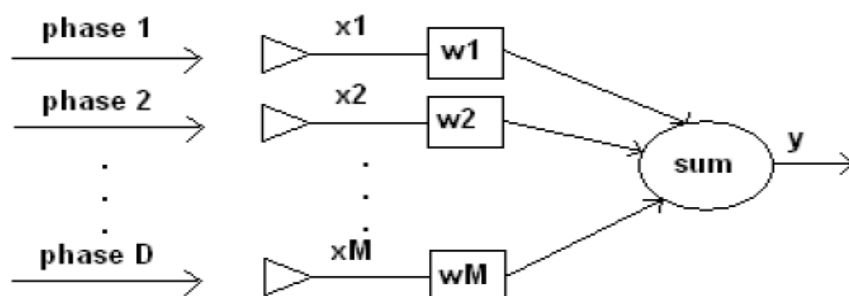$$\bar{w} = [w_1 \; w_2 \; w_3 \ldots . w_M] = array\ weights$$

Figure 5- M-elements array with arriving signals [3]

$$\bar{a}(\theta) = [1 \; e^{j(kd\sin\theta+\delta)} \; e^{j2(kd\sin\theta+\delta)} \; e^{j3(kd\sin\theta+\delta)} \; \ldots . e^{j(M-1)(kd\sin\theta+\delta)}]$$

$$s(k) = vector \; of \; incident \; complex \; monochromatic \; signals \; at \; time \; k.$$

$$\bar{n}(k) = noise \; vector \; at \; each \; array \; element, zero \; mean, variance \; \sigma_n^2.$$

$$\bar{a}(\theta_i) = M \; elements \; array \; steering \; vector \; for \; the \; \theta_i \; direction \; of \; arrivals.$$

The MxM array correlation matrix $\bar{R}_{xx}$ is given by

$$\bar{R}_{xx} = E[\bar{x}.\bar{x}^H]$$

$$\bar{R}_{xx} = E[(\bar{A}\bar{s} + \bar{n})(\bar{s}^H \bar{A}^H + \bar{n}^H]$$

$$\bar{R}_{xx} = \bar{A}E[(\bar{s}.\bar{s}^H)]\bar{A}^H + E[\bar{n}.\bar{n}^H]$$

$$\bar{R}_{xx} = \bar{A}\bar{R}_{ss}\bar{A}^H + \bar{R}_{nn}$$

Where

$$\bar{R}_{ss} = D \times D \; source \; correclation \; matrix$$

$$\bar{R}_{nn} = \sigma_n^2 \bar{I} = M \times M \; nosie \; correlation \; matrix$$

$$\bar{I} = N \times N \; identity \; matrix$$

The purpose of spectral estimation is to develop a function that gives an indication of the arriving angles based upon maxima vs. angle. This function is traditionally called the pseudospectrum and the units can be energy or in watts.

All the spectral estimation algorithms are based upon the pseudospectrum which gives an indication about the angle of arrival.

5.2 Spectral Estimation Algorithms

In [3] different spectral estimation algorithms are described in detail, some of these algorithms are explained here;

5.2.1 Capon Estimation

Capon estimation is also known as minimum variance distortion less response. The basic purpose of this algorithm is to maximize the signal to interference ratio (SIR), also considering the desired user as the main source and all power arriving from that direction while all other sources are considered as noise.

The maximized SIR is accomplished with set of array weights which are given as

$$\bar{w} = \frac{\bar{R}_{xx}^{-1}\bar{a}(\theta)}{\bar{a}^H(\theta)\bar{R}_{xx}^{-1}\bar{a}(\theta)}$$

The pseudospectrum of Capon estimation is given as

$$P_c(\theta) = \frac{1}{\bar{a}^H(\theta)\bar{R}_{xx}^{-1}\bar{a}(\theta)}$$

A major parameter on which the spectral estimation depends is the number of antenna elements. Figure 5.2 shows the plot for the above equation for six to eight and ten antenna elements signals arriving at -10^0 and 10^0.

As we increase the number of antennas, array steering vector and array correlation matrix size is increased accordingly, which improved the array resolution as shown is figure 5.2.

5.2.2 Bartlett Estimation

If the array is uniformly weighted, the Bartlett estimation can be defined as

$$P_B(\theta) = \bar{a}^H(\theta)\bar{R}_{xx}\bar{a}(\theta)$$

If we assume $\bar{s}$ represents uncorrelated monochromatic signals and there is no system noise, then the Bartlett estimation is equal to

$$P_B(\theta) = |\sum_{i=1}^{D}\sum_{m=1}^{M} e^{j(m-1)kd(\sin\theta - \sin\theta_i)}|^2$$

The beamwidth of antenna six antenna elements is almost 8.5^0, thus the two sources are 8.5^0or less apart are not resolvable. This is the limitation of Bartlett estimation. But array resolution can be improved by increasing the number of antenna element. Figure-5.3 shows the graph of Bartlett estimation with both the cases.
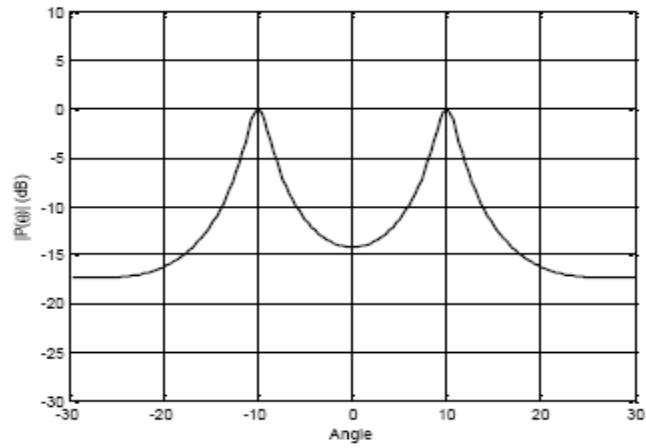
(a) Six antenna elements
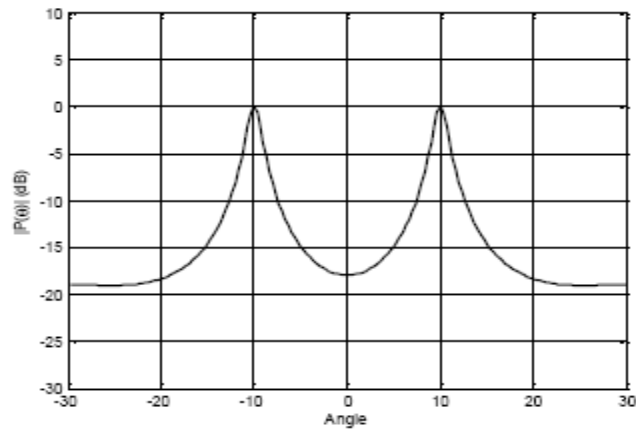
(b) Eight antenna elements
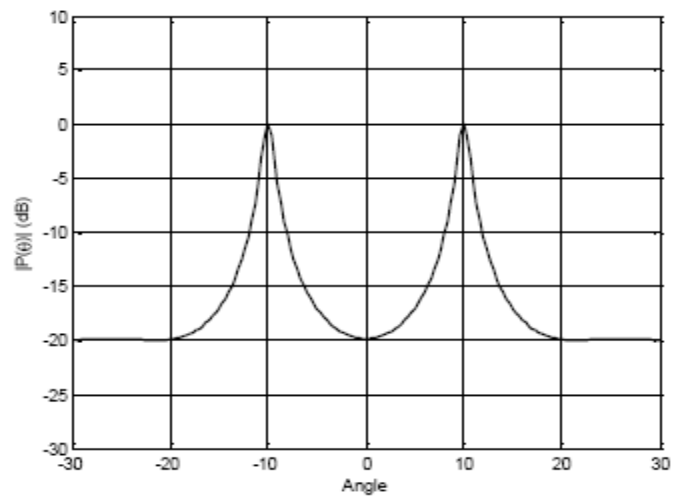
(c) Ten antenna elements

Figure 5- Capon Estimation
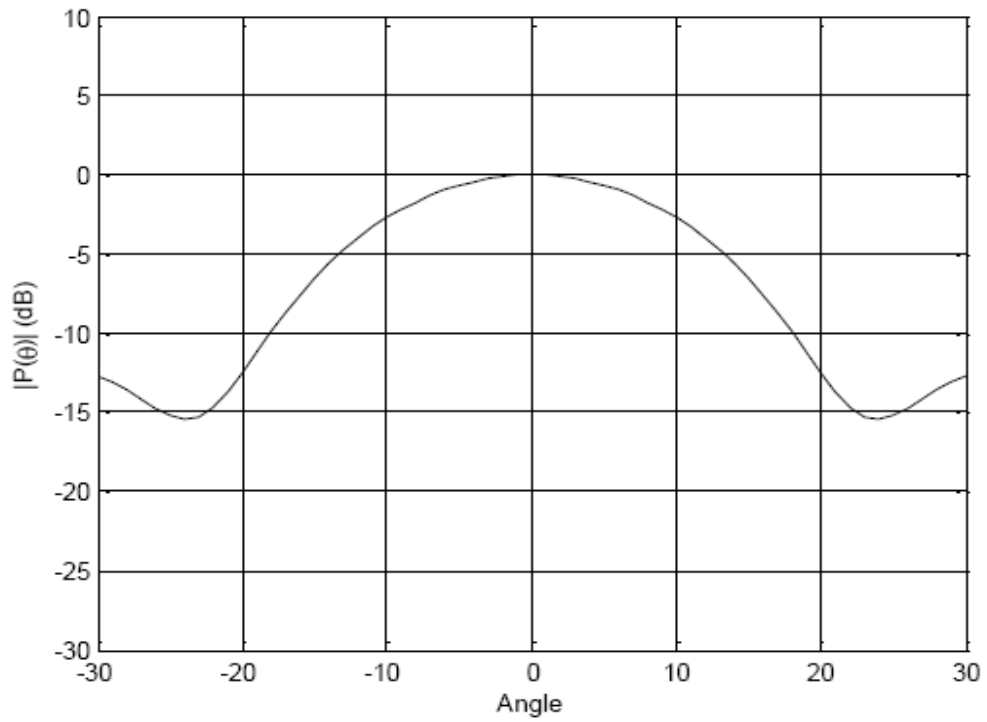
(a) Resolution of 10°
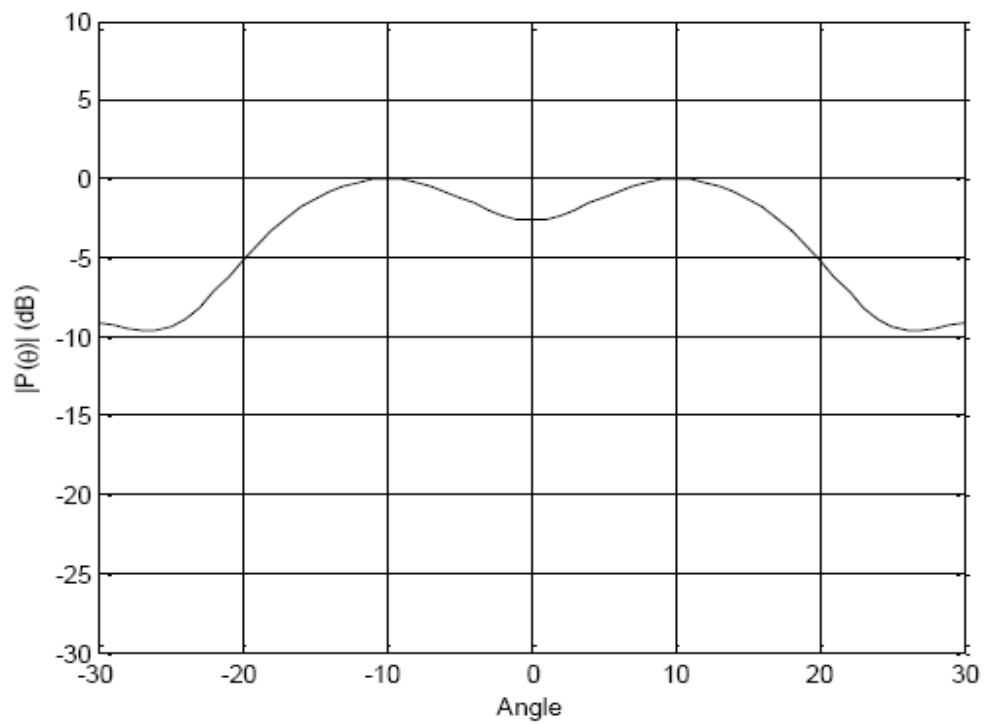
(b) Resolution of 20°

Figure 5- Bartlett Estimation

5.2.3 Linear prediction estimation

The common use of linear prediction estimation is to minimize the prediction error between the mth antenna element and the actual output. The goal is to find the appropriate weights that can minimize the mean-square prediction error. These weights can be found and given by

$$\bar{w}_M = \frac{\bar{R}_{xx}^{-1}\bar{u}_m}{u_m^T\bar{R}_{xx}^{-1}\bar{u}_m}$$

Where $\bar{u}_m$ is the Cartesian basis vector which is the mth column of the $M \times M$ identity matrix. The pseudo spectrum of linear prediction estimation is given by

$$P_{LP_m}(\theta) = \frac{u_m^T\bar{R}_{xx}^{-1}\bar{u}_m}{|u_m^T\bar{R}_{xx}^{-1}\bar{a}(\theta)|^2}$$

Figure 5.4 shows the plot for linear prediction estimation at 5^0 and -5^0.
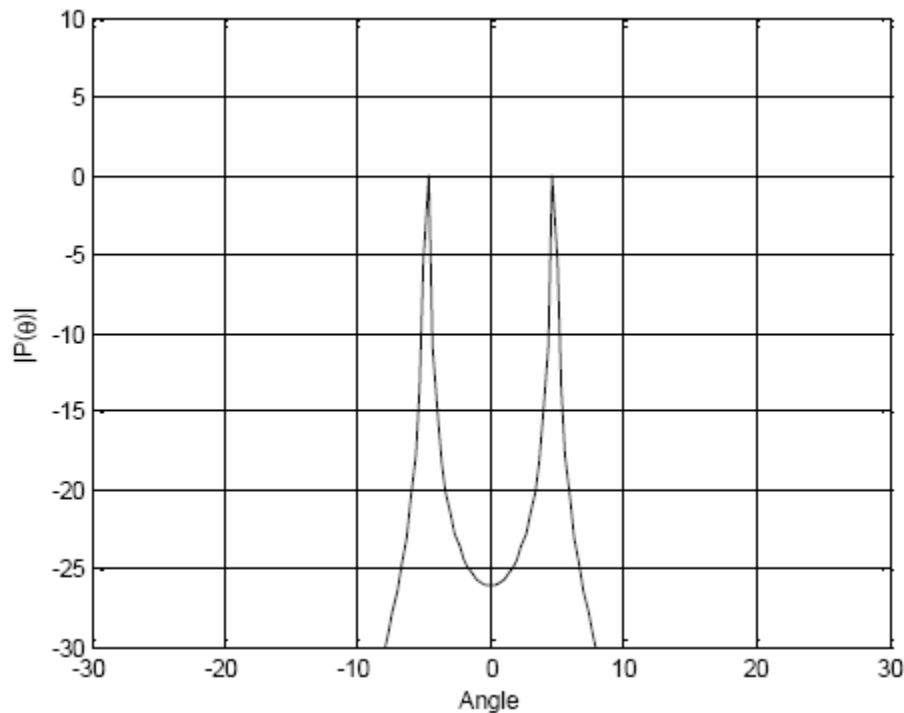
Figure 5- Linear prediction estimation

5.2.4 Maximum Entropy Estimation

The pseudospectrum of Maximum entropy estimation is given as

$$P_{ME_j} = \frac{1}{\bar{a}^H(\theta)\bar{c}_j\bar{c}_j^H\bar{a}(\theta)}$$

Where $\bar{c}_j$ is the jth column of the inverse correlation matrix $\bar{R}_{xx}^{-1}$. Figure 5.5 shows the plot of Maximum entropy estimation at 5^0 and -5^0.
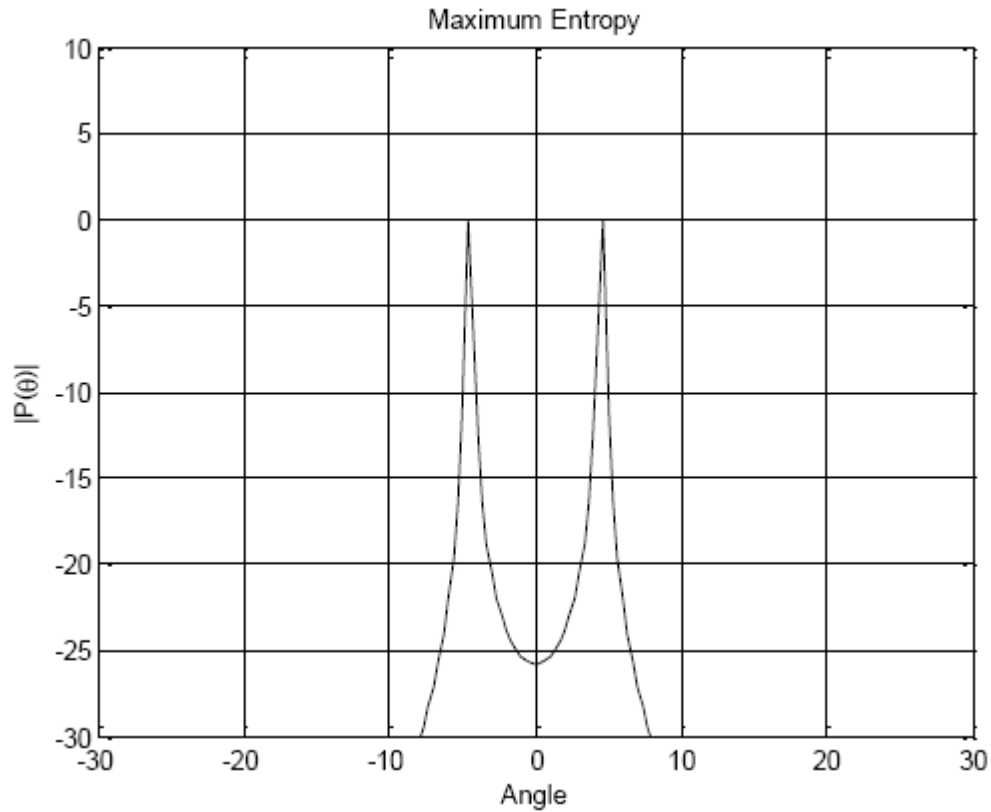
Figure 5- Maximum entropy estimation

5.2.5 Pisarenko Harmonic Decomposition Estimation

The Russian mathematician Pisarenko has proposed this algorithm. This is the minimum mean squared error approach similar to the linear predication estimation and goal is to minimize the mean squared error between the array output and actual output. It is given as

$$P_{PHD}(\theta) = \frac{1}{|\bar{a}^H(\theta)\bar{e}_1|^2}$$

Where $\bar{e}_1$ is the eigenvector associated with the smallest eigenvalue λ_1. This eigenvector $\bar{e}_1$ minimize the mean squared error corresponds to the smallest eigenvalue. For six antenna elements of array with two arriving signals, there will be two eigenvectors associated with the arriving signals and four eigenvectors are associated with noise.

Figure 5.6 shows the plot of Pisarenko harmonic estimation at 5^0 and -15^0. It can be shown that this estimation has accurate resolution.
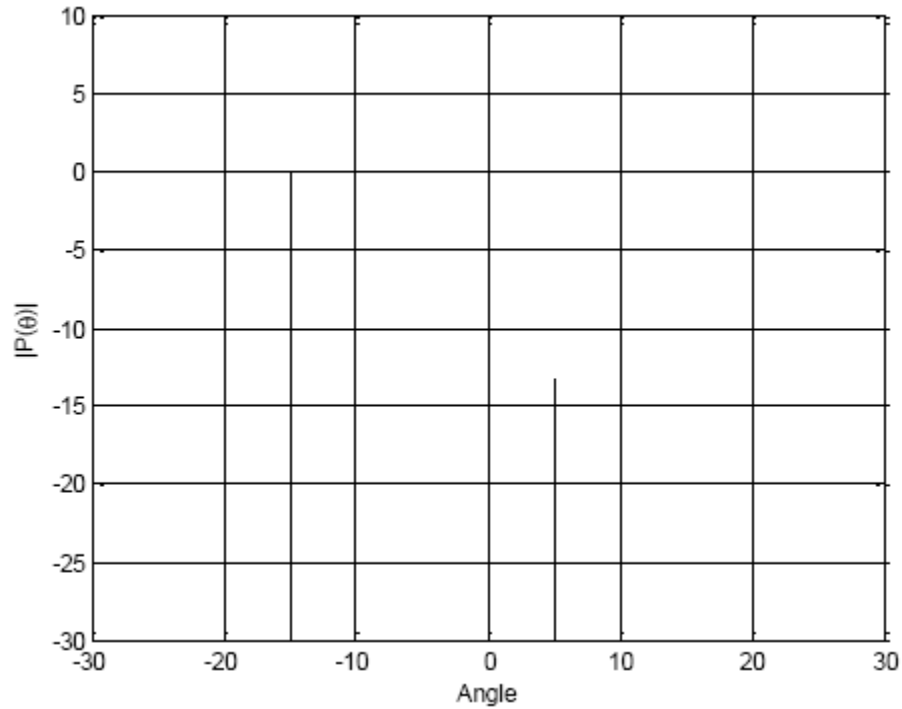
Figure 5- Pisarenko harmonic estimation

5.2.6 Minimum Norm Estimation

This method is developed by Reddi, Kumaresan and Tufts and also explained by Ermolaev and Gershman. The method is applicable for only uniform linear arrays. It is given as

$$P_{MN}(\theta) = \frac{(\bar{u}_1^T \bar{E}_N E_N^H \bar{u}_1)^2}{|\bar{a}^H(\theta) \bar{E}_N E_N^H \bar{u}_1|^2}$$

Where $\bar{E}_N$= subspace of $M - D$ noise eigenvectors $= [e_1 \ e_2 \ e_3 \ldots e_{M-D}]$

We can normalize the pseudospectrum of Min-norm as

$$P_{MN}(\theta) = \frac{1}{|\bar{a}^H(\theta) \bar{E}_N E_N^H \bar{u}_1|^2}$$

The Pisarenko harmonic estimation and Min-norm estimation are almost equal, the difference is that Pisarenko Harmonic method uses only first noise eigenvector whereas Min-norm combines all noise eigen vectors.

Figure 5.7 shows the plot for Min-norm estimation at 5 °and -15° .
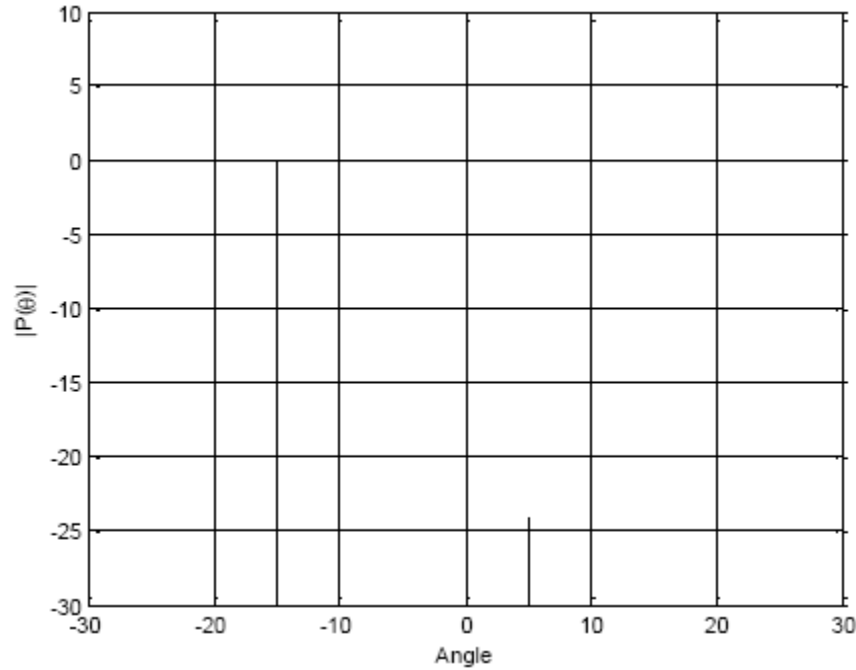
Figure 5- Min-norm estimation

5.2.7 MUSIC Estimation

MUSIC is the acronym of Multiple Signal Classification and like previous two algorithms MUSIC is also an Eigen structure algorithm. It is based on the assumption that the noise and the incoming signals are highly uncorrelated. The pseudospectrum is given as

$$P_{MU}(\theta) = \frac{1}{|\bar{a}^H(\theta)\bar{E}_N E_N^H \bar{a}(\theta)|}$$

Figure 5.8 shows the plot of MUSIC algorithm at 5^0 and -15^0.

In case where signals are correlated, plots can change dramatically and the resolution will diminish. Now we take the time samples of the received signal plus noise. The array correlation matrix is now defined as

$$\hat{R}_{xx} = E[\bar{x}(k).x^H(k)]$$

$$\hat{R}_{xx} \approx \frac{1}{K}\sum_{k=1}^{K} \bar{x}(k).x^H(k)$$

$$\hat{R}_{xx} \approx \bar{A}\hat{R}_{ss}\bar{A}^H + \bar{A}\hat{R}_{sn} + \hat{R}_{ns}\bar{A}^H + \hat{R}_{nn}$$

Where $\hat{R}_{ss} = \frac{1}{K}\sum_{k=1}^{K} \bar{s}(k).s^H(k)$ $\qquad$ $\hat{R}_{sn} = \frac{1}{K}\sum_{k=1}^{K} \bar{s}(k).n^H(k)$

$\hat{R}_{ns} = \frac{1}{K}\sum_{k=1}^{K} \bar{n}(k).s^H(k)$ $\qquad$ $\hat{R}_{nn} = \frac{1}{K}\sum_{k=1}^{K} \bar{n}(k).n^H(k)$
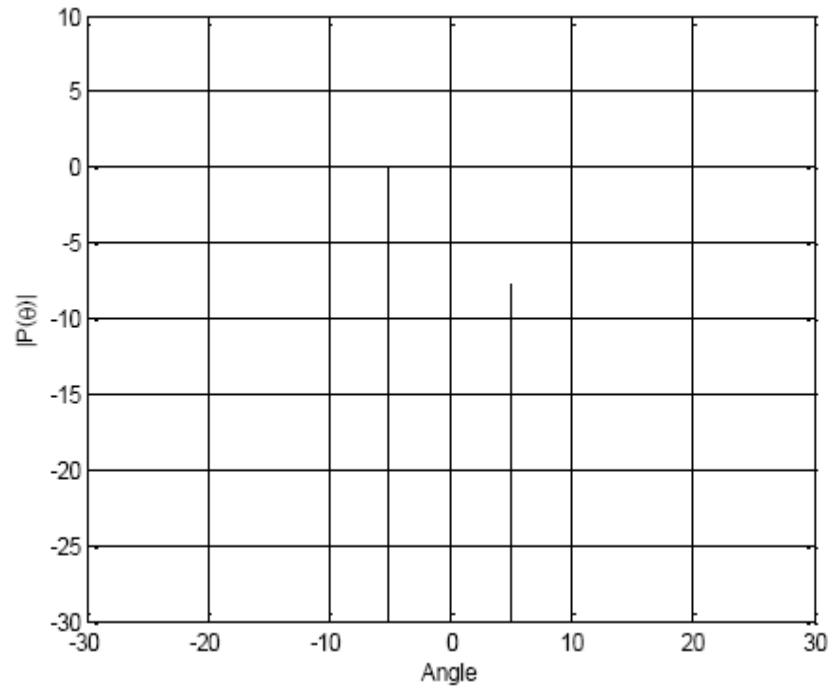
Figure 5- MUSIC estimation

Figure 5.9 shows the plot of time averages of MUSIC algorithm at 5^0 and -5^0.
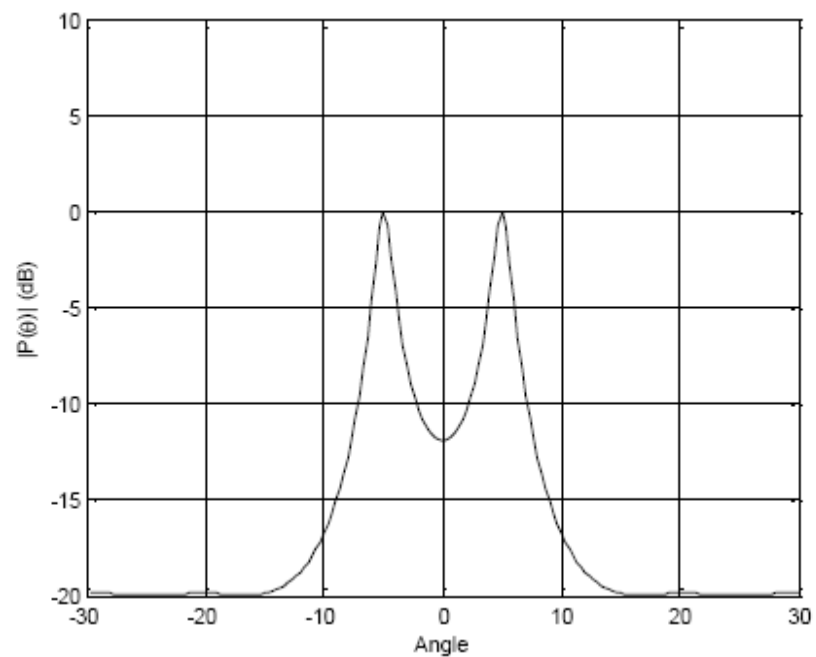
Figure 5- MUSIC estimation with time averages

5.3 <u>Beamforming</u>

In previous section different spectral estimation algorithms are discussed. The next goal is to direct the main beams towards the desired users and nulls towards interferes. This can be achieved using weighted array factor and finding the appropriate weights. There are mainly two different ways for finding these weights i.e. fixed beamforming and adaptive beamforming. [3]

5.3.1 Fixed Beamforming

5.3.1.1 A Simple Approach (Side Lobe Cancellation)

In this basic approach, we assume that the number of incoming signals is equal to number of antenna elements. Let us consider three elements array receiving exactly three signals, one is fixed desired source and other two are undesired interferers. The geometry of antenna array is linear with center at origin.

The array vector is thus given as

$$\bar{a} = \begin{bmatrix} e^{-jkd\sin\theta} \\ 1 \\ e^{jkd\sin\theta} \end{bmatrix}$$

And array weights are defined as

$$\bar{w}^H = [w_1 \; w_2 \; w_3]$$

The array output is given as

$$y = \bar{w}^H . \bar{a}$$

If the desired signals are at 0^0 and interferers are at 45^0 and 60^0, the weights are then calculated to be

$$\begin{bmatrix} w_1^* \\ w_2^* \\ w_3^* \end{bmatrix} = \begin{bmatrix} 0.28 - 0.07i \\ 0.45 \\ 0.28 + 0.07i \end{bmatrix}$$

By putting these weights in array factor, we get the plot as shown in figure below.
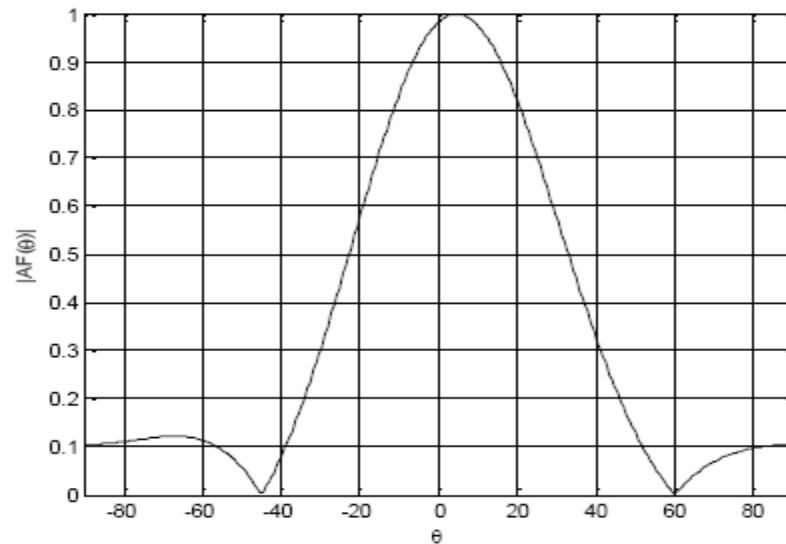
Figure 5- Sidelobe cancellation

5.3.2 Adaptive Beamforming

In case of mobile source signals angles of arrival will change with time. Therefore adaptive weighted algorithms are used to find the suitable weights. Some of adaptive beamforming techniques are

1. Least mean square
2. Sample matrix inversion
3. Recursive least squares etc.

CHAPTER 6

6   LITERATURE REVIEW AND RELATED WORK

In [13] Amir Anees and Omer Mujahid described organized approach to understand smart antenna system. A general overview of smart antenna is discussed in this paper. Array correlation matrix is discussed in this paper that is used for most DOA algorithms.
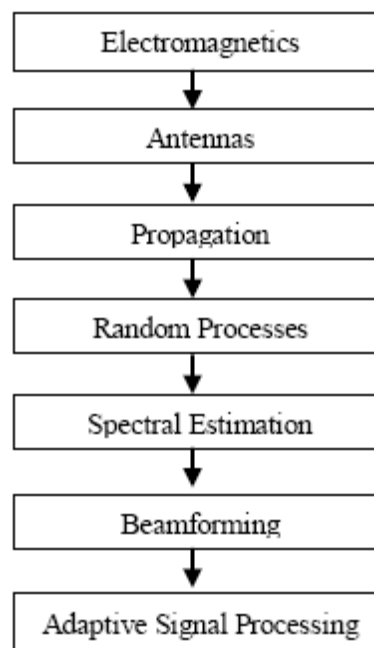
Figure 6- Approach to understand Smart Antenna

In [14] authors described CAPON and MUSIC techniques and compared the results for both by increasing the number of array elements. Simulation results show that if we increase the number of array elements CAPON and MUSIC resolution is improved.

$$P_c(\theta) = {}^1\!\big/\!{}_{\bar{a}^H(\theta)R_{xx}^{-1}\bar{a}(\theta)} \qquad\qquad P_{MU}(\theta) = {}^1\!\big/\!{}_{|\bar{a}^H(\theta)\bar{E}_N\bar{E}_N{}^H\bar{a}(\theta)|}$$

Also if we compare the figure 6.2 and figure 6.3, we will find that MUSIC algorithm resolution is more accurate than CAPON algorithm. However traditional MUSIC algorithms break down under high signal correlation.

a. Six antenna elements

b. Eight antenna elements

c. Ten antenna elements
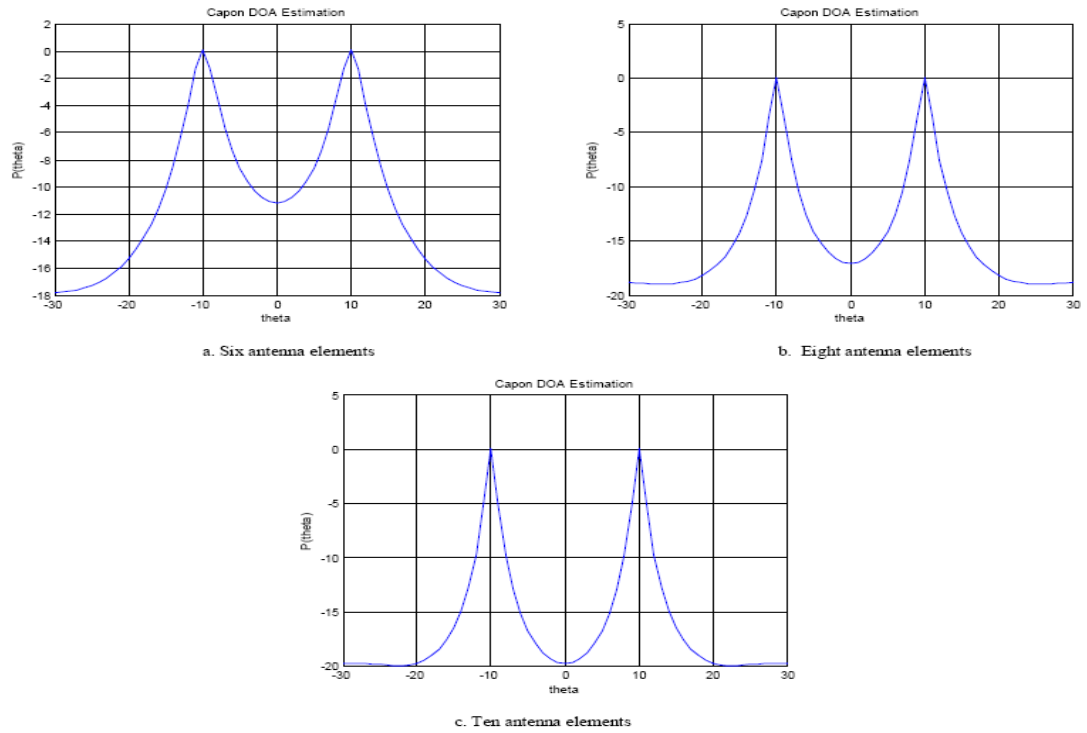
Figure 6- Capon Spectral Estimation

a. Six antenna elements

b. Eight antenna elements

c. Ten antenna elements
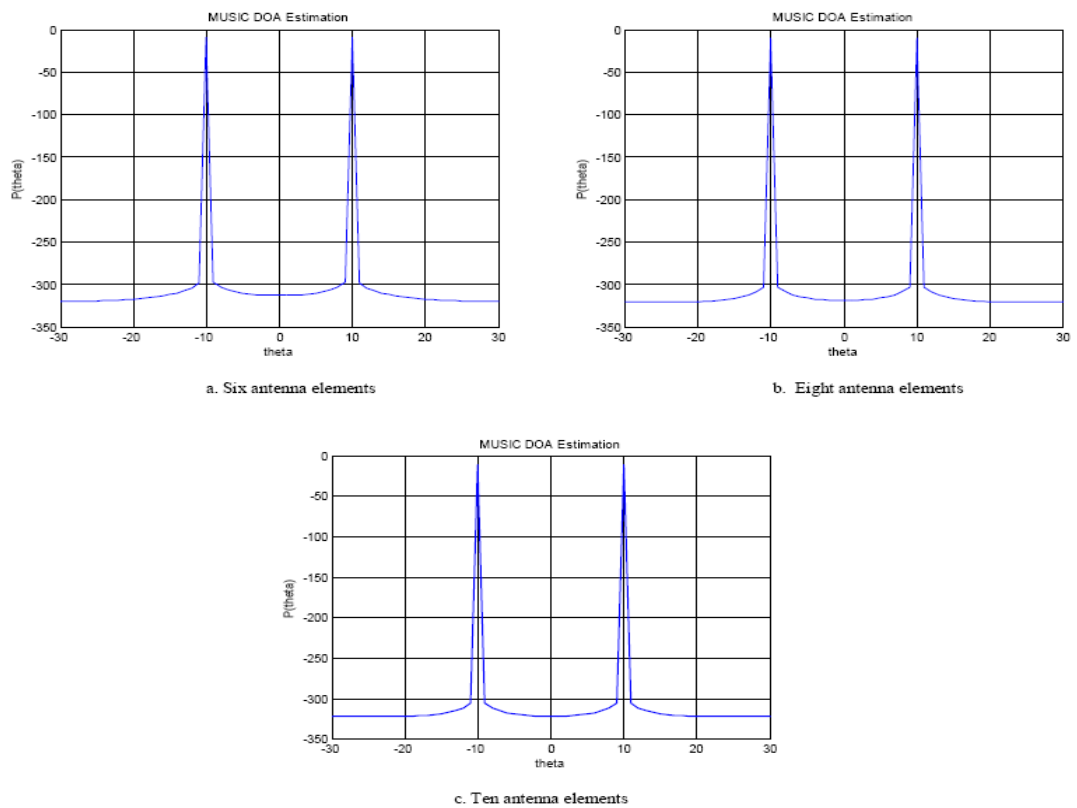
Figure 6- MUSIC Spectral Estimation

In [15] Dr.Md. Rafiq ul Islam and Ibrahim A.H Adam discussed Bartlett, MVDR, Linear prediction and MUSIC algorithms for ULA. MUSIC algorithm showed best resolution with minimum array elements and very small separation between angles of arrivals.

Spectral Estimation Algorithms Comparison:

Figure 6.4 shows the Bartlett simulation results for different angle of arrivals with different number of array elements. Sources with less than 10 degree separation are not resolved by using this algorithm. However we can improve resolution for desired signals by increasing the number of antenna elements.
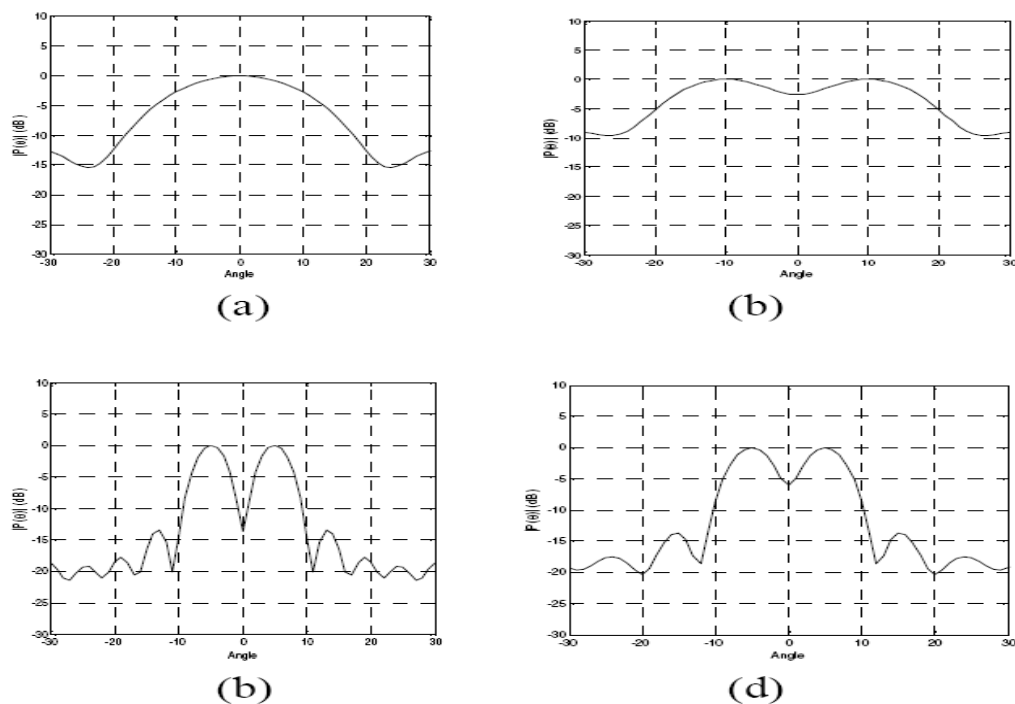
Figure 6- Bartlett Simulation (a) N=6, $\theta = \pm 5^{\circ}$ (b) N=6, $\theta = \pm 10^{\circ}$ (c) N=20, $\theta = \pm 5^{\circ}$ (d) N=20, $\theta = \pm 4^{\circ}$

MVDR is based on maximum likelihood estimation, in this method power of arriving signal is estimated and all other signals are considered as interference. MVDR has better resolution than Bartlett method. The fundamental goal of MVDR method is to increase the signal to interference ratio (SIR) and signal is passed with no effects signal phase and amplitude. For highly correlated signal sources CAPON (MVDR) method breaks down but if we consider the multipath signals with Rayleigh amplitude and uniform phase than uncorrelated condition is fulfilled and CAPON estimation algorithm works. Figure 6.5 shows the CAPON resolution with different number of antenna elements, N.
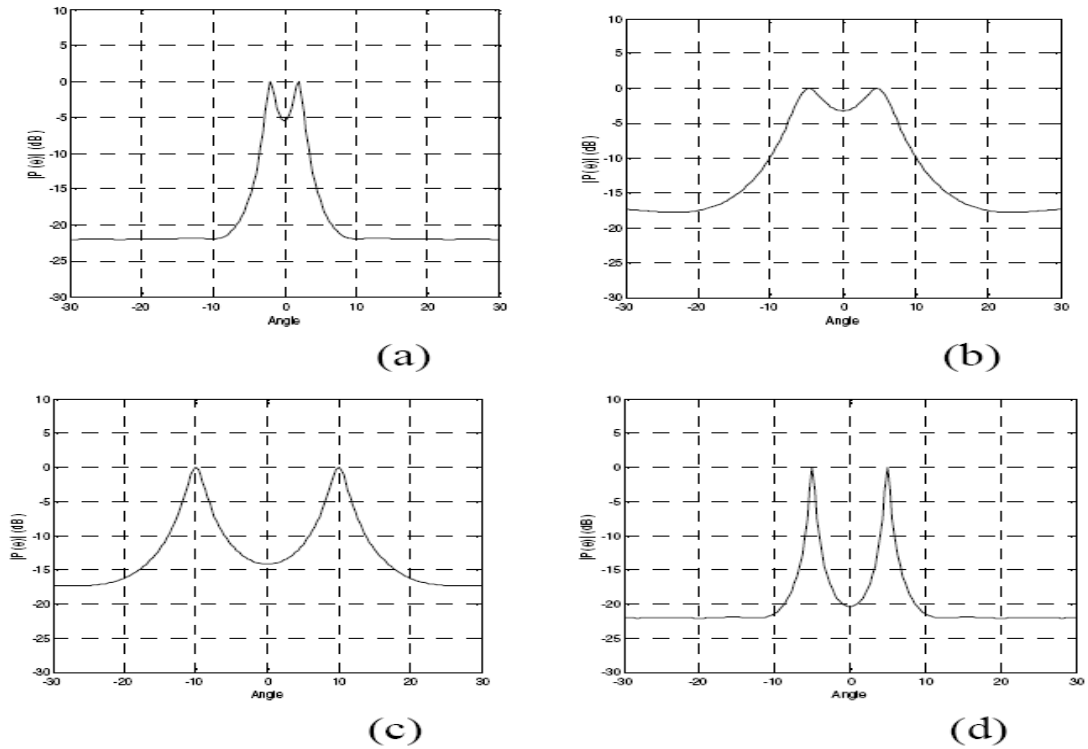
Figure 6- MVDR simulation (a) N=8, $\theta = \pm\,2^{\circ}$ (b) N=16, $\theta = \pm\,2^{\circ}$ (c) N=6, $\theta = \pm\,10^{\circ}$ (d) N=16, $\theta = \pm\,5^{\circ}$

Linear prediction algorithm has better results than both CAPON and Bartlett algorithms.
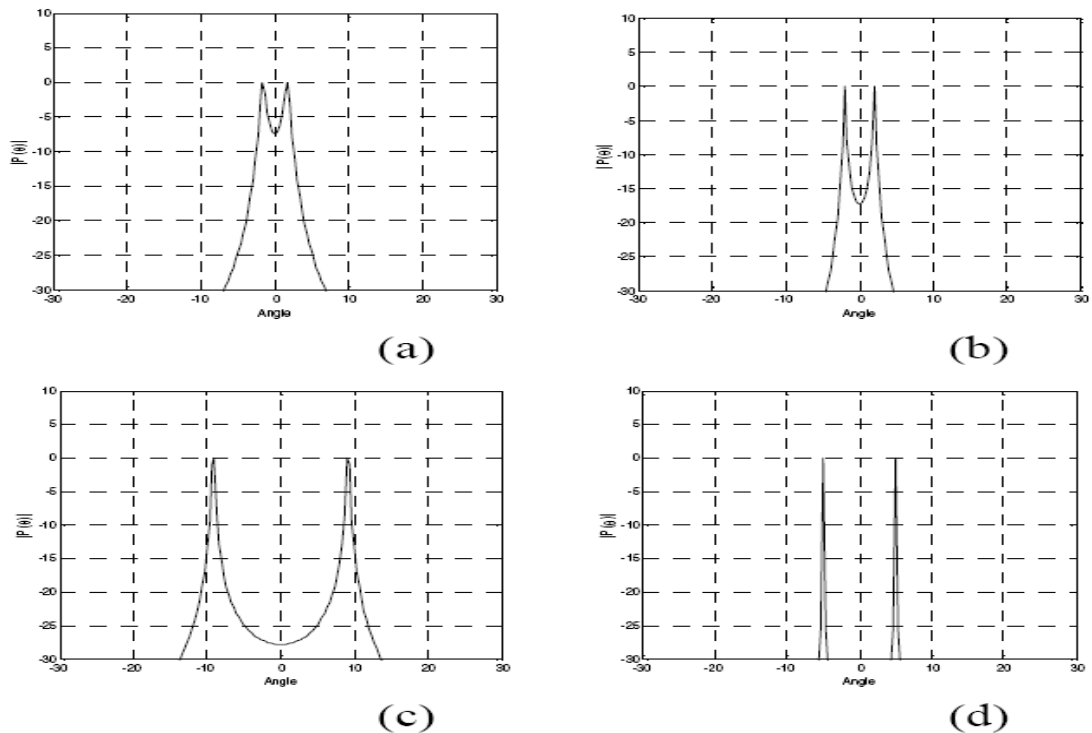
Figure 6- Linear Prediction Simulation (a) N=8, $\theta = \pm\,2^{\circ}$ (b) N=16, $\theta = \pm\,2^{\circ}$ (c) N=6, $\theta = \pm\,10^{\circ}$ (d) N=16, $\theta = \pm\,5^{\circ}$

MUSIC algorithm has best resolution as compared to Bartlett, CAPON and Linear prediction. This method is based on calculation of Eigen vectors and Eigen values. There are two subspaces in i.e. signal subspace and noise sub space. Noise sub space is used to estimate the spectrum of arriving signals. Also this method can resolve the angles arriving at even 1^0 separation.
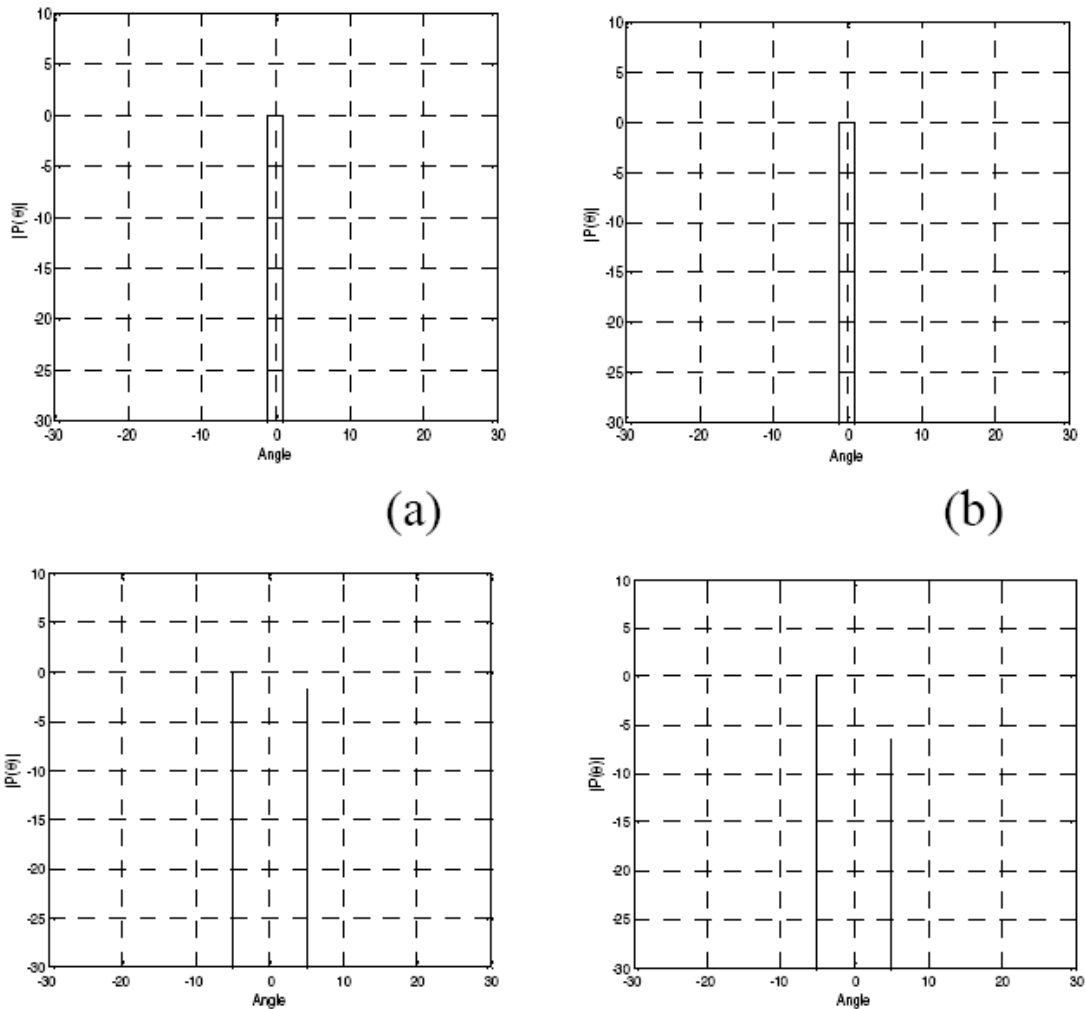

Figure 6- MUSIC Simulation (a) N=6, $\theta = \pm\, 1^{\circ}$ (b) N=16, $\theta = \pm\, 1^{\circ}$ (c) N=6, $\theta = \pm\, 5^{\circ}$ (d) N=16, $\theta = \pm\, 5^{\circ}$

In [16] Suchita W.Varade, K.D Kulat used seven element array with interspacing $\frac{\lambda}{2}$ and compared the results of MUSIC and MVDR algorithms with two interference signals and different angle of arrivals. Table-1 shows the simulation results.

Table Simulation Results

User 1	User2	User3	real direction	calculated direction		error	
				MUSIC	MVDR	MUSIC	MVDR
10	20	30	20.0	19.85	19.87	0.15	0.13
0	10	20	0	1.1	0	1.1	-
0	70	90	90.0	90.1	90	0.1	-

In [17] Raymond J. Weber* and Yikun Huang compared CAPON and MUSIC algorithms with variable array length. MUSIC algorithm has better performance than CAPON estimation.

The mean square error is defined as:

$$MSE = \sum_{n=1}^{N} \frac{(\hat{\phi}_n - \phi)^2}{N - 1}$$
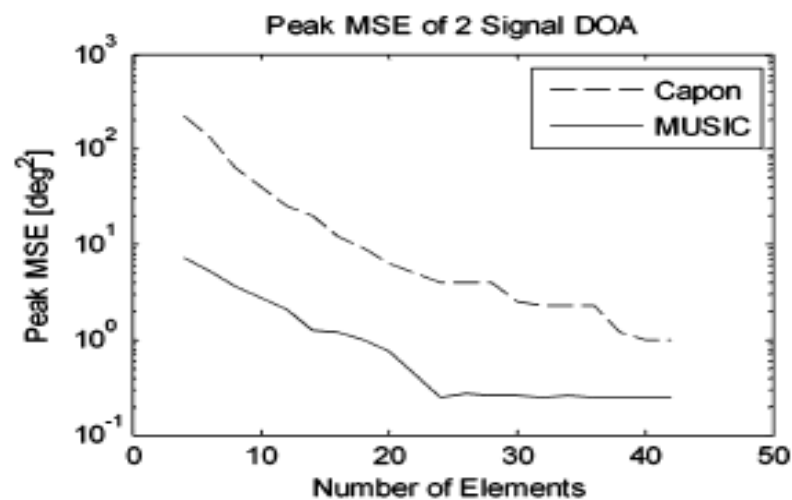
Figure 6- Phase error for two independent, equal power signals vs. number of sensors m.

In [18] authors described MUSIC and ESPRIT DOA techniques by varying following parameters;

1. Number of antenna elements N= 5,11 (computational load increases with N)
2. Number of snapshots K=10 to 100
3. SNR -20dB to 20dB

$$SNR = 10log_{10}\left(\frac{\sigma_s^2}{\sigma_N^2}\right) \; with \; \bar{R}_s = E[\bar{s}.\bar{s}^H] = \sigma_s^2\bar{I}_M$$

MUSIC is more stable than ESPRIT algorithm under above conditions and has better results.

In [19] E M AI-Ardi, R M Shuhair and M E Al-Mualla described MUSIC and ESPRIT algorithms. It was found that these algorithms performance improves by addressing below factors;

1. Angular separation between incident signals
2. Separation between ULA elements. (Must be less than 0.5λ)
3. SNR
4. Number of snapshots K=50 to 500
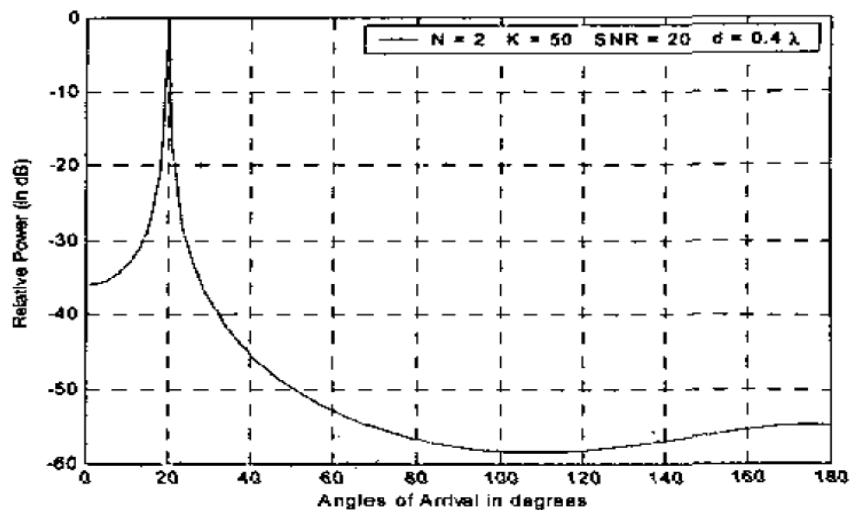
(a)   Element spacing d=0.4λ
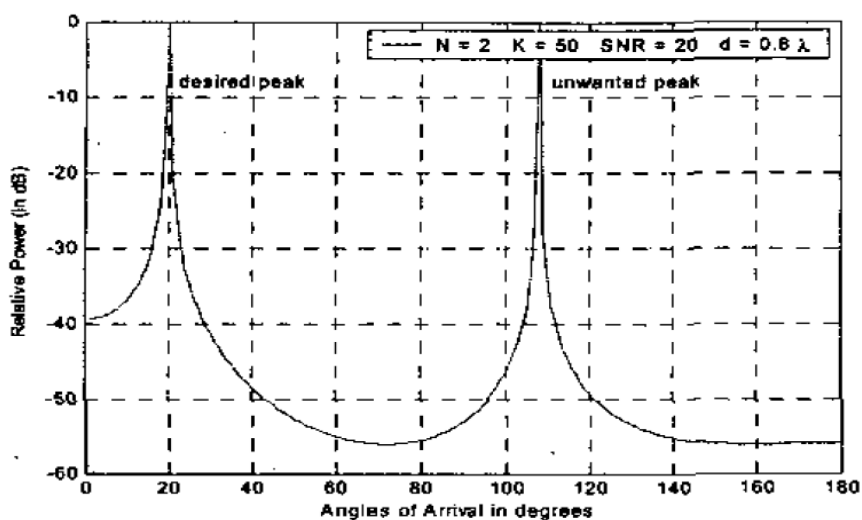
Figure 6- Effects of increasing array elements spacing for desired signal at 20 degree

Spectral Estimation Algorithm for Smart Antenna Systems

In [20] WO BU discussed uniform circular arrays using MUSIC algorithm, also a comparison is made with Bartlett algorithm. As compared to MUSIC, Bartlett algorithm failed to resolve 0, 20 and 40 degree angles.

The array response vector of uniform circular array is given by

$$a(\theta_k) = \begin{bmatrix} e^{j2\pi(^r/_\lambda)\cos(\theta_k)} \\ e^{j2\pi(^r/_\lambda)\cos(\theta_k - \frac{1}{M}2\pi)} \\ . \\ . \\ e^{j2\pi(^r/_\lambda)\cos(\theta_k - \frac{(M-1)}{M}2\pi)} \end{bmatrix}$$
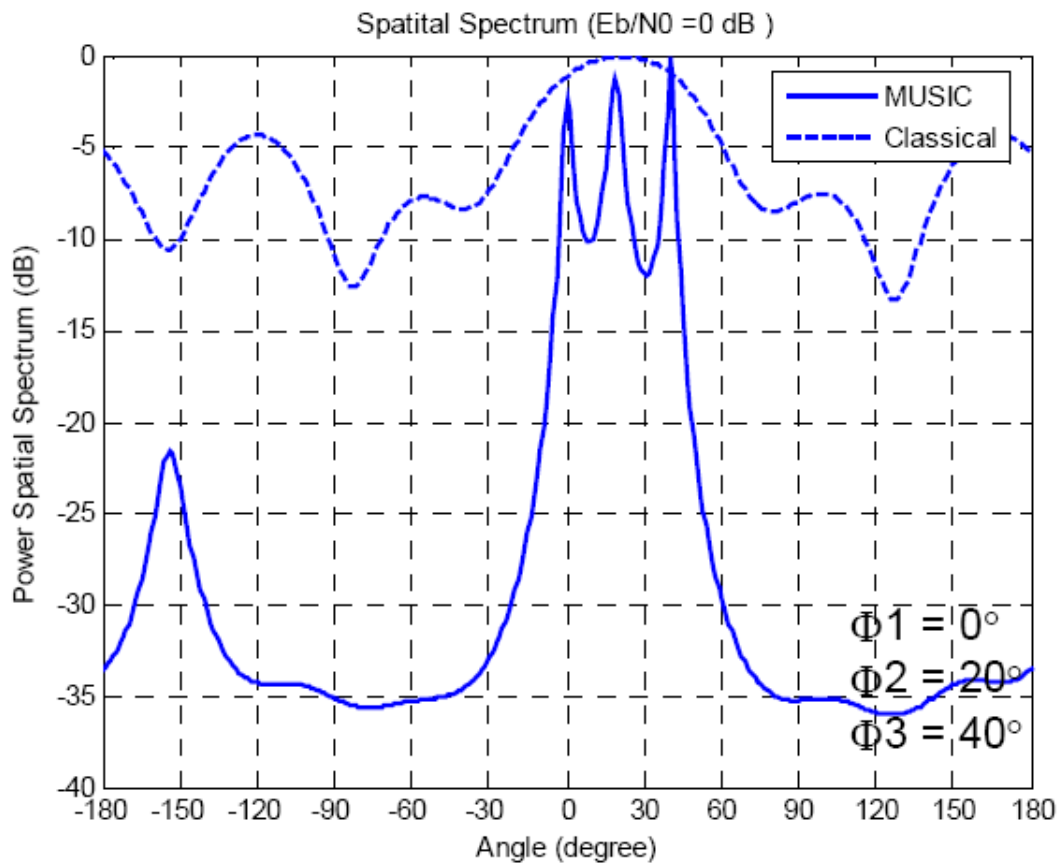
Figure 6- MUSIC and Bartlett simulation

In [21] R.M Shubair and R.S Al Nuaimi describes displaced sensor array (DSA) technique to resolve narrow band sources at grazing incident directions with high resolution. DSA consists of two ULA parallel arrays as shown is figure 6.11. User signal vector for m incident direction is given by

$$x(t) = \sum_{m=1}^{M} [a_1(\theta_m) + a_2(\theta_m)]S_m(t) + n(t)$$

Where n(t) is Gaussian noise vector with zero mean. $a_1(\theta_m)$ and $a_2(\theta_m)$ are array steering vectors for both ULA elements in DSA arrangement with respect to θ_m angles of arrival.

Where

$$a_1(\theta_m) = [e^{[j(n-1)\psi_m]}]^T; \; \psi_m = 2\pi(\frac{d}{\lambda}) \sin \theta_m \;\; 1 \le n \le N$$

And

$$a_2(\theta_m) = a_1(\theta_m).F_s(\theta_m).F_\Delta(\theta_m)$$

Where $F_s(\theta_m)$ and $F_\Delta(\theta_m)$ represents the space factor due to vertical separation s and horizontal separation Δ.

$$F_s(\theta_m) = e^{-j2\pi(\frac{S}{\lambda}) \cos \theta_m}$$

$$F_\Delta(\theta_m) = e^{-j2\pi(\frac{\Delta}{\lambda}) \sin \theta_m}$$

The array steering vectors are given by

$$A_1 = [a_1(\theta_1) \; a_1(\theta_2) \; a_1(\theta_3) \dots a_1(\theta_M)]$$

$$A_2 = [a_2(\theta_1) \; a_2(\theta_2) \; a_2(\theta_3) \dots a_2(\theta_M)]$$

The received signal vector is given by

$$x(t) = [A_1 + A_2]s(t) + n(t) = As(t) + n(t)$$
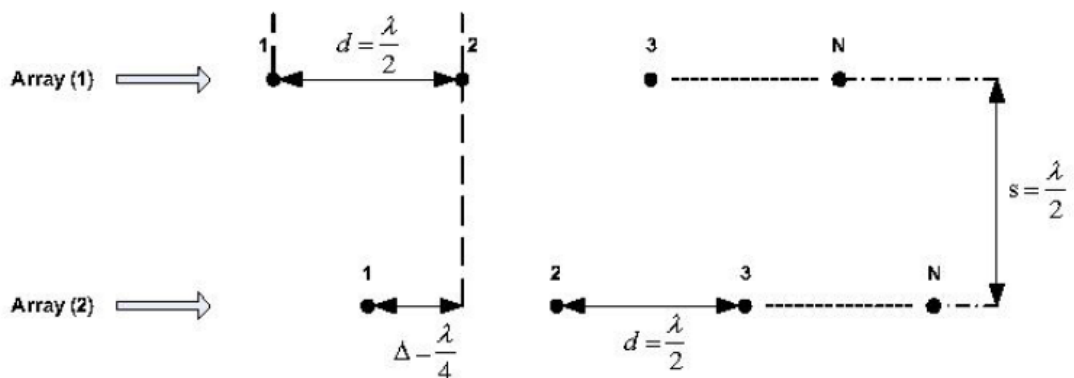
Figure 6- Displacement Sensor Array configuration

Now the correlation matrix is given by

$$R = E[x(t)x^H(t)]$$

If we use time average the spatial correlation matrix is given by

$$R = \frac{1}{K} \sum_{k=1}^{K} x(k) x^H(k)$$

$$R = A R_{ss} A^H + n(k) n^H(k)$$

Where $R_{ss} = E[s(t)s^H(t)]$ is an M×M source correlation matrix.

Simulation results are shown in figure 6.12 for MUSIC algorithm for ULA with N=4 elements and proposed DSA with 2N=8

SNR= 20dB

Snapshots = K=1000

Grazing incident angles $\theta_1 = -75^0 \ and \ \theta_2 = 75^0$
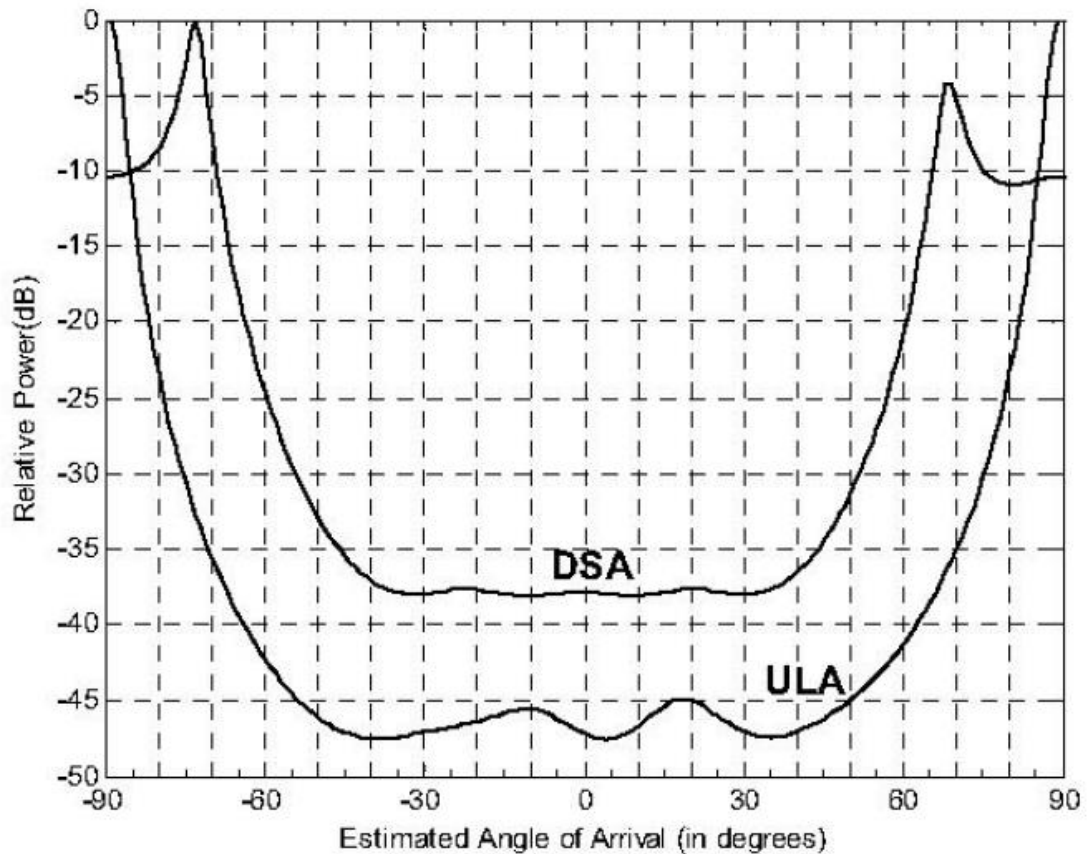
Figure 6- MUSIC algorithm for ULA and DAS for $\boldsymbol{\theta_1 = -75^{\circ} \ and \ \theta_2 = 75^{\circ}}$

CHAPTER 7

7 PROPOSED SPECTRAL ESTIMATION ALGORITHM FOR SMART ANTENNA SYSTEMS

7.1 Problem Statement

Wireless channel characteristics changes due to environmental conditions like noise, interference etc. Fixed beamwidth antenna systems not provide the optimum solution because its beam is not properly directed to the signals of interest. Fixed beam antenna transmits in a specific direction and cannot change its characteristics with user movement and interference signals reduce the quality of service and capacity. So, smart antennas are introduced to increase the capacity, bandwidth and QoS. Signal to noise ratio (SNR), signal power, gain, beam width, robustness and convergence to desired signals is improved by using different spectral estimation and adaptive beamforming algorithms. Spectral estimation is of prime importance to find the direction of arriving signals and direct main beam of smart antenna toward desired users. There are different spectral estimation algorithms to find the direction of desired incoming signals i.e. Bartlett, CAPON, Linear Prediction, Minimum Norm and MUSIC etc. MUSIC algorithm supports many array configurations. For uniform linear array (ULA) MUSIC is one of the best spectral estimation algorithms but it cannot resolve sources located at close angles towards the array endfire direction.

To overcome this problem modified ULA is proposed. By simply adding two more elements in ULA setup array resolution and accuracy can be improved.

7.2 Proposed Solution

Figure 7.1 shows the block diagram of smart antenna system. It consists of ULA with N antenna elements, D arriving signals and N-D interference signals.

Figure 7- Block diagram of smart antenna system[22]

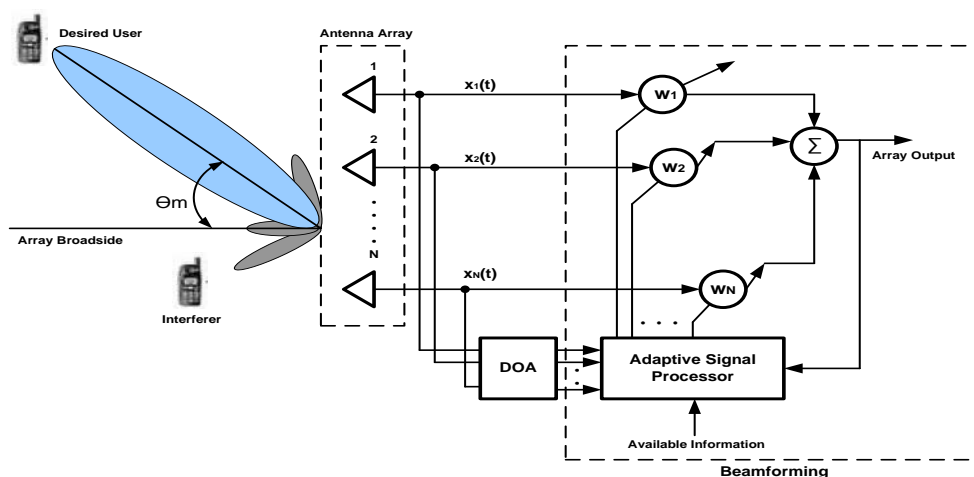Spectral estimation is basic part of smart antenna system which finds the direction of arrival of desired signals and passes it to adaptive signal processor for beamforming.

7.2.1 Spectral Estimation Techniques

7.2.1.1 Capon Estimation

Capon estimation is also known as minimum variance distortion less response. The basic purpose of this algorithm is to maximize the signal to interference ratio (SIR), also considering the desired user as the main source and all power arriving from that direction while all other sources are considered as noise.

The maximized SIR is accomplished with set of array weights which are given as

$$\bar{w} = \frac{\bar{R}_{xx}^{-1}\bar{a}(\theta)}{\bar{a}^H(\theta)\bar{R}_{xx}^{-1}\bar{a}(\theta)}$$

The pseudo spectrum of Capon estimation is given as

$$P_c(\theta) = \frac{1}{\bar{a}^H(\theta)\bar{R}_{xx}^{-1}\bar{a}(\theta)}$$

A major parameter on which the spectral estimation depends is the number of antenna elements.

7.2.1.2 Bartlett Estimation

If the array is uniformly weighted, the Bartlett estimation can be defined as

$$P_B(\theta) = \bar{a}^H(\theta)\bar{R}_{xx}\bar{a}(\theta)$$

If we assume $\bar{s}$ represents uncorrelated monochromatic signals and there is no system noise, then the Bartlett estimation is given by

$$P_B(\theta) = |\sum_{i=1}^{D}\sum_{m=1}^{M} e^{j(m-1)kd(\sin\theta - \sin\theta_i)}|^2$$

7.2.1.3 MUSIC Estimation

MUSIC is the acronym of Multiple Signal Classification and like previous two algorithms MUSIC is also an Eigen structure algorithm. It is based on the assumption that the noise and the incoming signals are highly uncorrelated. The pseudo spectrum is given as

$$P_{MU}(\theta) = \frac{1}{|\bar{a}^H(\theta)\bar{E}_N E_N^H \bar{a}(\theta)|}$$

7.2.2 Uniform Linear Array Setup

A simplest ULA is shown is figure 7.2 with N array elements uniformly spaced with distance $d = \frac{\lambda}{2}$. Arriving signals are assumed uncorrelated and in line of sight with zero mean Gaussian noise and variance σ_n^2. The input signal vector is given by

$$x(t) = AS + n$$

Where A is M×D matrix of array steering vectors $a(\theta_m)$ and given by

$$A = [a(\theta_1)\ a(\theta_2)\ a(\theta_3)\ .....\ a(\theta_M)]$$

The MxM array correlation matrix $\bar{R}_{xx}$ is given by

$$\bar{R}_{xx} = E[\bar{x}.\bar{x}^H]$$

$$\bar{R}_{xx} = E[(\bar{A}\bar{s} + \bar{n})(\bar{s}^H\bar{A}^H + \bar{n}^H]$$

$$\bar{R}_{xx} = \bar{A}E[(\bar{s}.\bar{s}^H)]\bar{A}^H + E[\bar{n}.\bar{n}^H]$$

$$\bar{R}_{xx} = \bar{A}\bar{R}_{ss}\bar{A}^H + \bar{R}_{nn}$$

Where

$$\bar{R}_{ss} = D \times D\ source\ correclation\ matrix$$

$$\bar{R}_{nn} = \sigma_n^2\bar{I} = M \times M\ nosie\ correlation\ matrix$$

$$\bar{I} = N \times N\ identity\ matrix$$

Now array correlation matrix is given by

$$\bar{R}_{xx} = \bar{A}\bar{R}_{ss}\bar{A}^H + \sigma_n^2\bar{I}$$

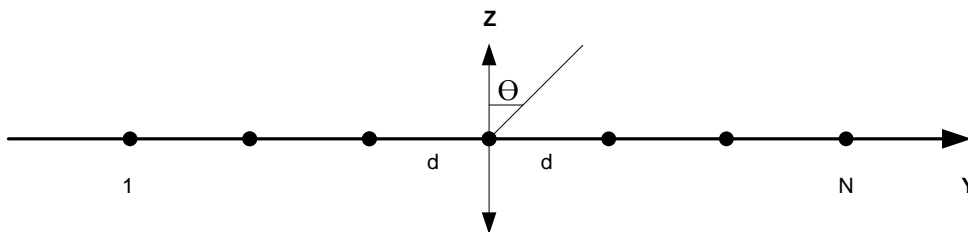This array correlation matrix is used in many spectral estimation algorithms like Bartlett, CAPON and MUSIC etc.

Figure 7- Uniform Linear Array

$$a_{ULA}(\theta_m) = \left[e^{[j(n-1)\psi_m]}\right]^T$$

Where $\psi_m = 2\pi\left(\frac{d}{\lambda}\right)\sin\theta_m$ for $1 \leq n \leq N$

The array steering vector for ULA is N×1 vector and for N=5 given by

$$a_{ULA}(\theta_m) = \begin{bmatrix} 1 \\ e^{jkd\sin\theta_m} \\ e^{j2kd\sin\theta_m} \\ e^{j3kd\sin\theta_m} \\ e^{j4kd\sin\theta_m} \end{bmatrix}$$

Where $d = \frac{\lambda}{2}$ and $k = \frac{2\pi}{\lambda}$ and λ is wavelength of arriving signals.

Major advantages of ULA are its simplicity, narrow beam width and high directivity as compared to other array setups. However ULA does not resolve all the incident angle of arrivals especially for sources that are closed to array endfire. DSA is one setup that can resolve the grazing incident angle of arrivals [21]. This problem can also be resolved by using other array setups but it leads to complication. This drawback of ULA can be resolved by modifying the ULA and adding just two elements in ULA setup.

7.2.3 Modified Uniform Linear Array

Modified uniform linear array setup is shown in figure 7.3 with N+2 linear elements equally spaced with $d = \frac{\lambda}{2}$ and centered at origin.
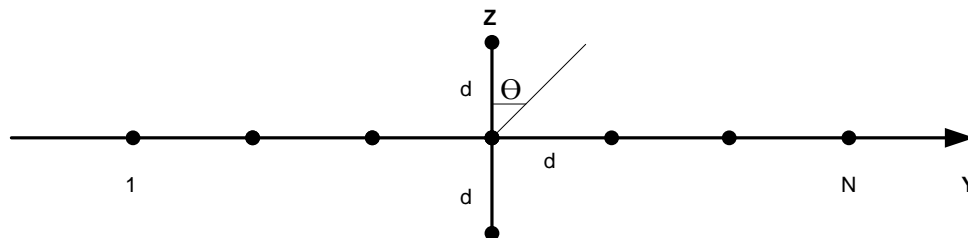
Figure 7-3 Modified ULA

The array steering vectors for modified ULA M × 1 vector is given by, where M=N+2

$$x(t) = \sum_{m=1}^{M}[a_1(\theta_m) + a_2(\theta_m)]S_m(t) + n(t)$$

$$a_1(\theta_m) = \left[e^{-j\left[\left(\frac{n-1}{n}\right)-n\right]\psi_m}\right]^T \text{ For } 1 \leq n \leq N$$

Where ψ_m is the electrical phase shift from element to element and given by

$$\psi_m = 2\pi(\frac{d}{\lambda})\sin\theta_m$$

For $d = \frac{\lambda}{2}$ & $\lambda = \frac{2\pi}{K}$

$$\psi_m = kd \sin \theta$$

For N = 5 linear array elements

$$a_1(\theta_m) = \begin{bmatrix} e^{-2jkd \sin \theta_m} \\ e^{-jkd \sin \theta_m} \\ 1 \\ e^{jkd \sin \theta_m} \\ e^{2jkd \sin \theta_m} \end{bmatrix}$$

For two extra elements along z-axis array vector is given by [21]

$$a_2(\theta_m) = a_1(\theta_m) \times F_s(\theta_m) \times F_\Delta(\theta_m)$$

Where $F_s(\theta_m)$ and $F_\Delta(\theta_m)$ represent the space factors due vertical separation 's' and horizontal displacement 'Δ'.

With $\pm d = \frac{\lambda}{2}$, $\Delta = 0$ & $n = 1$

$$a_2(\theta_m) = \begin{bmatrix} e^{jkd \cos \theta_m} \\ e^{-jkd \cos \theta_m} \end{bmatrix}$$

So,

$$a_{M-ULA}(\theta_m) = \begin{bmatrix} e^{-j2kd\sin\theta_m} \\ e^{-jkd\sin\theta_m} \\ 1 \\ e^{jkd\sin\theta_m} \\ e^{jkd\sin\theta_m} \\ e^{jkd\cos\theta_m} \\ e^{-jkd\cos\theta_m} \end{bmatrix}$$

Where $d = \frac{\lambda}{2}$ and $k = \frac{2\pi}{\lambda}$ and λ is wavelength of arriving signals. First five elements is array steering vector are from ULA and last two are due to two elements added as shown in modified ULA. And array matrix is given by

$$A = [A_1 + A_2]$$

7.3 Simulations and Results

Array resolution and accuracy of Bartlett, Capon and MUSIC algorithms is compared in both ULA and modified ULA with ULA having N=5 elements and modified ULA having M=N+2=7 elements centered at origin. It is assumed that signals are uncorrelated with inter element spacing $d = \frac{\lambda}{2}$ and number of snapshots K=1000. Two sources close to array boresight and two sources close to array endfire direction are considered to determine the array resolution and accuracy.

Simulations result show that the spectrum of Bartlett algorithms using both array setups failed to resolve all the directions of arrival.
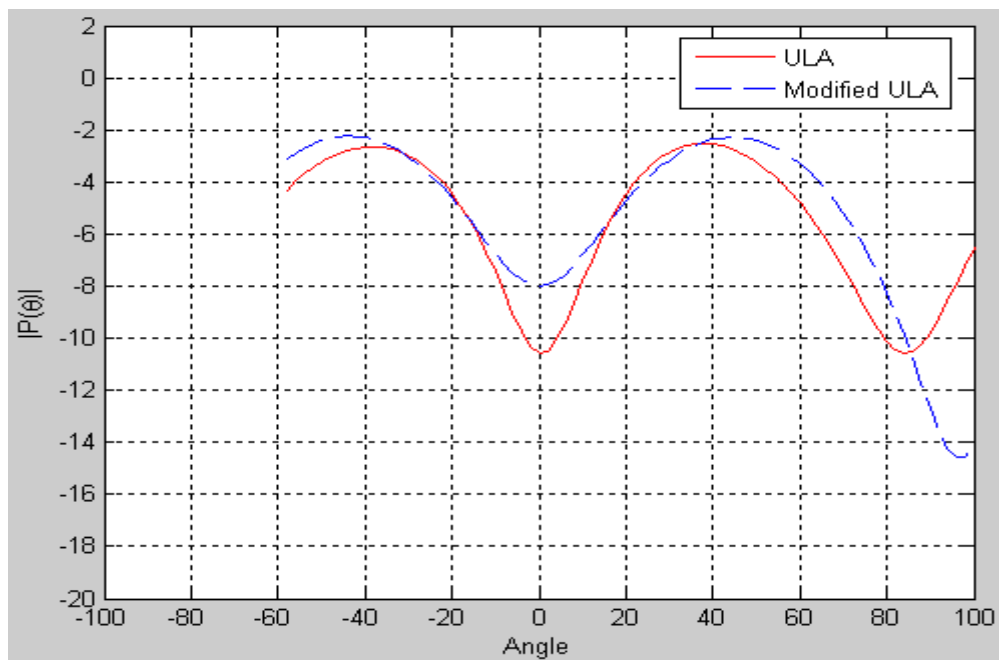
Figure 7- Bartlett Spectrum for ULA and Modified ULA with sources at -20°, 20°, 80°, 85°

Figure 7.4 shows the spectrum of CAPON algorithm for both ULA and modified ULA. As from figure first three angles are resolved by both array setups but Modified array has more sharp peeks than ULA setup. Also Modified ULA setup resolves all angles arriving at endfire direction. Below table summarize the simulations results, ULA setup is only efficient for sources located at array boresight but modified ULA setup is more accurate towards array endfire and also has better or similar array resolution for middle angles.
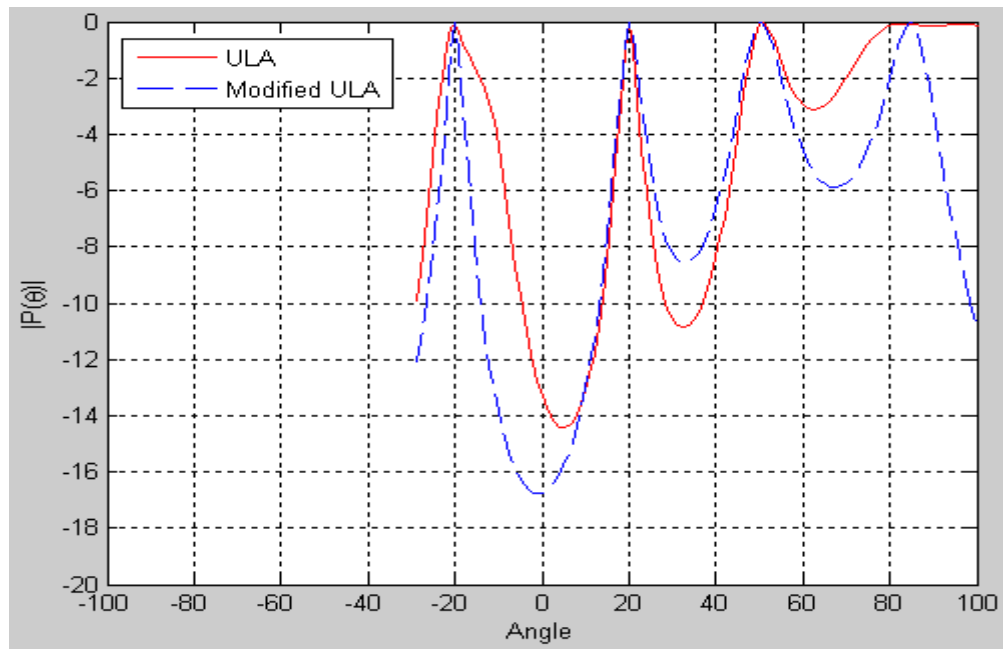
Figure 7- CAPON Spectrum for ULA and Modified ULA with sources at -20°, 20°, 50°, 85°

Table 2 Simulation Results

Arriving Angles (Degree)	Actual DOA	Capon Estimated DOA		Capon Efficiency	
		ULA	Modified ULA	ULA	Modified ULA
θ1	-5°	-5°	No Result	100%	0%
θ2	5°	5°	No Result	100%	0%
θ3	45°	42°	41°	93%	91%
θ4	70°	69°	68°	99%	97%
θ1	-10°	-10°	-10°	100%	100%
θ2	10°	10°	10°	100%	100%
aθ3	50°	51°	52°	98%	96%
θ4	75°	72°	74°	96%	99%
θ1	-20°	-20°	-20°	100%	100%
θ2	20°	20°	20°	100%	100%
θ3	55°	58°	56°	95%	98%
θ4	80°	No Result	79°	0%	99%
θ1	-25°	-25°	-25°	100%	100%
θ2	25°	25°	25°	100%	100%
θ3	60°	68°	57°	88%	95%
θ4	85°	No Result	79°	0%	93%

Figure 7-5 shows the spectrum of MUSIC algorithm for both ULA and Modified ULA under similar angles of arriving conditions to CAPON.
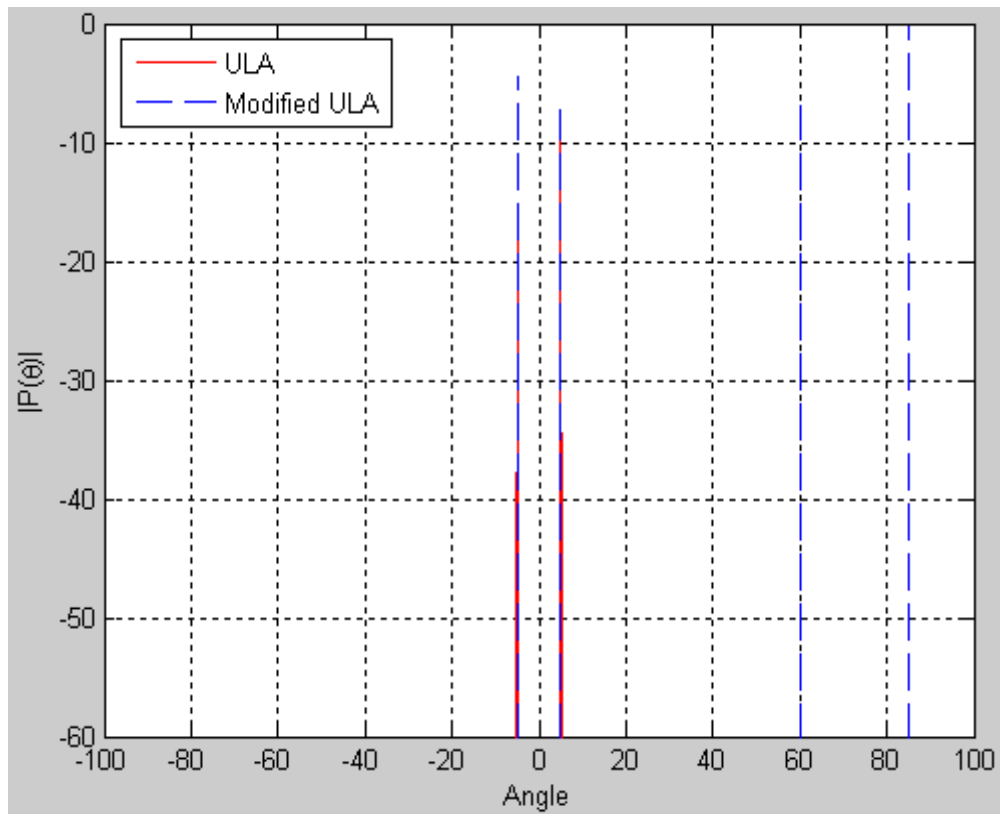
Figure 7- MUSIC Spectrum for ULA and Modified ULA with sources at -5°, 5°, 60°, 85°

Modified ULA accurately resolves all the angle of arrival including the sources arriving in array endfire direction.

Table 3 Simulation Results

Arriving Angles (Degree)	Actual DOA	MUSIC Estimated DOA		MUSIC Efficiency	
		ULA	Modified ULA	ULA	Modified ULA
θ1	-1°	-1°	-1°	100%	100%
θ2	1°	1°	1°	100%	100%
θ3	45°	No Result	45°	0%	100%
θ4	70°	No Result	70°	0%	100%
θ1	-10°	-10°	-10°	100%	100%
θ2	10°	10°	10°	100%	100%
θ3	50°	No Result	50°	0%	100%
θ4	75°	No Result	75°	0%	100%
θ1	-20°	-20°	-20°	100%	100%
θ2	20°	20°	20°	100%	100%
θ3	75°	No Result	75°	0%	100%
θ4	80°	No Result	80°	0%	100%
θ1	-25°	-25°	-25°	100%	100%
θ2	25°	25°	25°	100%	100%
θ3	85°	No Result	85°	0%	100%
θ4	95°	No Result	95°	0%	100%

ULA setup resolves the angles close to array boresight but fail to resolve angles arriving in endfire direction. However Modified ULA setup accurately resolves all the angle of arrival including the endfire directions.

All the simulation results are analyzed using MATLAB tool and spectral estimation algorithms codes are available in separate CD with thesis.

Chapter 8

8   Conclusion

Smart antenna systems are one of the most promising technologies, which play vital role in improving the overall efficiency of wireless communication. Smart antenna systems help in interference cancellation, SNR improvement due to antenna gain and multipath mitigation which improve coverage, capacity and QoS. In this thesis, modified ULA has been presented for spectral estimation of smart antenna systems to resolve the sources located towards array endfire direction. Modified ULA has been integrated with different spectral estimation algorithms i.e. CAPON, Bartlett and MUSIC and results are compared with ordinary ULA setup under same configurations. ULA setup resolves the angles close to array boresight but fail to resolve angles arriving in endfire direction. However Modified ULA setup accurately resolves all the angle of arrival including the endfire directions. It has been found that array resolution and accuracy has been improved with modified ULA setup. Also complexity and overall hardware cost has been reduced as number of array elements has not been increased to improve the array resolution.

References:

[1] Van Atta, L. "Electromagnetic Reflection," U.S Patent 2908002, Oct. 6, 1959

[2] Howells, P. "Intermediate Frequency Sidelobe Canceller," U.S. Patent 3202990, Aug.24,1965

[3] Frank Gross, "Smart Antennas for wireless communication with MATLAB book" Patent 0-07-144789-X

[4] JHON D.KRAUS, "ANTENNAS second edition book" 1988 by McGraw Hill, Inc.

[5] Balanis, C. Antenna Theory Analysis and Design, Wiley, 2d ed., New York, 1997.

[6] Kraus, J., and R. Marhefka, Antennas for All Applications, 3d ed., McGraw-Hill, New York, 2002.

[7] Peng Liang, "Shenzhen Winhap Main Passive Materials Specificatons" Jan 5 2007

[8] Balanis,C.,Antenna Theory: Analysis and Design,2d ed., Wiley, New York,1997.

[9] Harris, F.J "One the Use of Windows for Harmonic Analysis with DFT," IEEE Proceedings, pp.51-83,Jan 1978

[10] Nuttall, A.H., "Some Windows with Very Good Sidelobe Behavior," IEEE Transactions on Acoustics,Speech, and Signal Proceeding, Vol. ASSP-29, No.1, Feb.1981

[11] Keller, J.B., "Geometrical Theory of Diffraction," J. Opt. Soc. Amer., Vol. 52, pp. 116-130, 1962

[12] Rappaport, T.S., Wireless Communications: Principles and Practice, 2d ed., Prentice Hall, New York,2002

[13] Amir Anees, Umer Mujahid, "A Systematic Approach to Understand Smart Antenna" 28 March 2011

[14] Amir Anees, Umer Mujahid, Dr Jameel Ahmed,Waseem Altaf, "Spectral Estimation Algorithms for Smart Antenna Systems" 4 April 2011

[15] Dr. Md Rafiqul Islam, Ibrahim A.H Adam, "Performance Study of Direction of Arrival (DOA) Estimation Algorithms for Linear Array Antenna" 2009 International Conference on signal Processing Systems.

[16] Suchita W.Varade, K.D. Kulat, "Robust Algorithms for DOA Estimation and Adaptive Beamforming for Smart Antenna" Second International Conference on Engineering and Technology,ICETET-09

[17] Raymond J.Weber* , Yikun Huang, "Analysis for Capon and MUSIC DOA Estimation algorithms" 978-1-4244-3647-7/09/$25.00©2009IEEE

[18] T.B. LAVATE, Prof. V.K. KOKATE,Prof. Dr. A.M.SAPKAL, "Performance Analysis of MUSIC and ESPRIT DOA Estimation algorithms for adaptive array smart antenna in mobile communication" Second International Conference in Computer and Network Technology

[19] EM Al-Ardi, R M Shuhair, ME Al-Mualla, "INVESTIGATION OF HIGH-RESOLUTION DOA ESTIMATION ALGORITHMS FOR OPTIMAL PERFORMANCE OF SMART ANTENNA SYSTEM" 0 2003, the institution of

Electrical Engineers. Printed and published by the IEE, Michael Faraday House, Six Hills Way, Stevenage. SG1 ZAY

[20]   Wu Bo, "Realization and Simulation of DOA estimation using MUSIC Algorithm with Uniform Circular Arrays" CEEM'2006/Dalian 4A5-08

[21]   R.M Shubair, R.S Al Nuaimi, "A DISPLACEMENT SENSOR ARRAY CONFIGURATION FOR ESTIMATING ANGLES OF ARRIVAL OF NARROWBAND SOURCES UNDER GRAZING INCIDENCE CONDITIONS" 2007 IEEE International Conference on Signal Processing and Communications (ICSPC2007), 24-27 November 2007, Dubai, United Arab Emirates